


RESEARCH

Open Access



Seismic vulnerability assessment of residential buildings using logistic regression and geographic information system (GIS) in Pleret Sub District (Yogyakarta, Indonesia)

Aditya Saputra^{1,2*} , Trias Rahardianto^{1,3}, Mohamad Dian Revindo^{4,5}, Ioannis Delikostidis¹, Danang Sri Hadmoko⁶, Junun Sartohadi⁶ and Christopher Gomez⁷

Abstract

Background: The Southeast of Yogyakarta City has had the heaviest damages to buildings in the 2006 of Yogyakarta Earthquake disaster. A moderate to strong earthquake of 6.3 Mw shook the 20 km southeast part of the Yogyakarta City early in the morning at 5:54 local time. On top of extensive damage in Yogyakarta and Central Java, more than 5700 people perished; 37,927 people were injured in the collapse of more than 240,396 residential buildings. Furthermore, the earthquake also affected the infrastructure and local economic activities. The total damages and losses because of the earthquake was 29.1 trillion rupiahs or equal to approximately 3.1 million US dollar. Two main factors that caused the severe damages were a dense population and the lack of seismic design of residential buildings. After reconstruction and rehabilitation, the area where the study was conducted grew into a densely populated area. This urbanistic change is feared to be potentially the lead to a great disaster if an earthquake occurs again. Thus, a comprehensive study about building vulnerability is absolutely needed in study area. Therefore, the main objective of this study has been the provision of a probabilistic model of seismic building vulnerability based on the damage data of the last big earthquake. By considering the relationship between building characteristics, site conditions, and the damage level based on probabilistic analysis, this study can offer a better understanding of earthquake damage estimation for residential building in Java.

Results: The main findings of this study were as follows: The most vulnerable building type is the reinforced masonry structure with clay tile roof, it is located between 8.1-10 km of the epicentre and it is built on young Merapi volcanic deposits. On the contrary, the safest building type is the houses which has characteristics of reinforced masonry structure, asbestos or zinc roof type, and being located in Semilir Formation. The results showed that the building damage probability provided a high accuracy of prediction about 75.81%.

Conclusions: The results explain the prediction of building vulnerability based on the building damaged of the Yogyakarta earthquake 2006. This study is suitable for preliminary study at the region scale. Thus, the site investigation still needs to be conducted for the future research to determine the safety and vulnerability of residential building.

Keyword: Earthquake, Damage pattern, Building vulnerability, Probabilistic model

* Correspondence: aditya.saputra@pg.canterbury.ac.nz;
aditsaputra1987@gmail.com

¹Department of Geography, University of Canterbury, Private Bag 4800,
Christchurch, New Zealand

²Geography Faculty, Universitas Muhammadiyah Surakarta, Central Java,
Indonesia

Full list of author information is available at the end of the article

Background

An earthquake is a sudden motion of the earth caused by the release of accumulated energy that mostly occurs within or along the edges of earth's tectonic plates. The released energy generates the seismic vibration radiating in the earth's body and perceived as an earthquake (Bath, 1979). This natural phenomenon strongly relates to the geological condition and the configuration of tectonic plates. The areas located at the edges of tectonic plates are more vulnerable to earthquake hazard. However, few earthquakes can also occur away from the tectonic plates boundary such as in the interior of a tectonic plate or intraplate regions (Stein & Wysession, 2003).

Indonesia is an archipelago country located between three active tectonic plates: The Pacific Plate, the Eurasian Plate, and the Indo-Australian Plate. Demets et al. (1994) and Schluter et al. (2002) stated that the Eurasian Plate is relatively more stable than the other two tectonic plates. The Pacific Plate is moving northward with an average velocity of 11–12.5 cm/year while the Indo-Australian Plate is moving 7.23 cm/year westward. According to U.S. Geological Survey (USGS), at least 14,000 earthquakes greater than 5.0 Richter occurred in this area between 1900 and 2009 with the biggest earthquake (9.1 MW) having occurred in the Andaman Sea, west coast of Aceh (northern Sumatra) on 26 December 2004. The Andaman earthquake also generated a destructive tsunami and caused massive casualties not only in Indonesia but also in other nations surrounding the Indian Ocean such as Sri Lanka, India, Thailand, Somalia, Myanmar, Maldives, etc. The other big earthquakes occurred in Indonesia after Aceh Earthquake 2004 were Nias Earthquake in 2005 (Mw = 8.7), Yogyakarta Earthquake in 2006 (Mw = 6.3), Tasikmalaya Earthquake in 2009 (Mw = 7.4), Padang earthquake in 2009 (Mw = 7.6), and Kebumen, Central Java Earthquake in 2014 (Mw = 6.1) (Irsyam, et al., 2010).

Yogyakarta earthquake on May 27th, 2006, was unexpected not only for Yogyakarta residents but also for all Indonesians. A moderate to strong, 6.3Mw earthquake hit Yogyakarta early in the morning at 5:54 local time. According to USGS, the epicentre was located 20 km Southeast of Yogyakarta City at geographic coordinates 7.9620°S, 110.4580°E. This earthquake caused extensive damage in Yogyakarta and Central Java. More than 5,700 people died, 37,927 people were injured, and 240,396 residential buildings were destroyed, and the local infrastructure and economic activities were largely disrupted. According to the damage assessment conducted in June 2006, the cost of damage and losses reached 29.1 trillion rupiahs (US\$ 3.1 million). This made the Yogyakarta earthquake one of the worst disasters in Indonesia in the last ten years (BAPPENAS 2006).

Housing was the most severely impacted sector, with more than half of the total private building stocks of 2004 being affected and an estimated total loss of about 15.3 trillion rupiahs. The impacts on other sectors such as infrastructure, lifeline, and trade were widespread but relatively limited in severity. For example, the Pedan electricity substation was switched off directly after earthquake. Three sets of 500KV circuit breakers, five sets of 500KV and two sets of 500 KV/150KV electricity transformers, and a 500KV lighting arrester suffered significant damages. Social, education and productive sectors also experienced significant damage due to the earthquake. At least 2,155 school buildings, 17 private hospitals, 41 private clinics and 45 health clinics (*PUSKESMAS*) were destroyed, and the same happened with as many as 2,201 religious facilities (20% of their total number in 2004). Additionally, a large number of enterprises, mostly small and mid-sized ones, such as shops and traders, were completely damaged. Furthermore, several main traditional markets such as Niten, Imogiri, Pleret and Piyungan were closed. The summary of estimated damages and losses in infrastructure and productive sectors are shown in Table 1 while the details about affected small and medium enterprises can be seen in Table 2.

Two primary factors that caused the severe damages were the high density of population in the affected areas (1,600 people per km²) and the lack of seismic design of housing units (Elnashai et al., 2006). Before 2006, the house types in Yogyakarta and its suburbs, could be divided into three categories: 1) unreinforced masonry or URM (in older houses, i.e., pre-1990), 2) partially reinforced masonry (newer houses, post-1990) and 3)

Table 1 The summary of damage and losses in infrastructure and productive sectors (Billion Rp)

Sectors or sub-sectors	Damages	Losses	Total
Energy			
Electricity transmission	135	150	285
Water supply			
PDAM water supply	5.0	3.7	8.7
Rural water supply	75.5	0	75.5
Transport and communication			
Roads	45	0	45
Railways	19.9	0	19.9
Civil Aviation	18.7	0.2	18.9
Post and Telecoms	7.0	0	7.0
Agriculture			
Production	0	638.4	638.4
Irrigation infrastructure and storage facilities	44	0	44
Fish ponds, fish stock	13.2	1.4	14.6

Source: (BAPPENAS 2006)

Table 2 The summary of directly affected units of SMEs due to the earthquake on 27 May, 2006

Name of affected district	Number of SMEs (pre disaster)	Affected units			Workers in SMEs		Dependents on formal SMEs	Total Affected
		Formal	Informal	Total	Formal	Informal		
Bantul	21,306	9,588	5,040	14,628	335,570	20,160	1,342,278	1,362,438
Klaten	25,000	4,500	3,360	7,860	157,500	13,440	630,000	643,440
Kodya Yogyakarta	8,619	776	1,680	2,456	27,150	6,720	108,599	115,319
Sleman	18,558	1,113	1,120	2,233	38,972	4,480	155,887	160,367
Gunungkidul	21,659	650	560	1,210	22,742	2,240	90,968	93,208
Kulonprogo	22,418	673	560	1,233	23,539	2,240	94,156	96,396
Total	117,560	17,299	12,320	29,619	605,472	49,280	2,421,888	2,471,168

Source: (BAPPENAS 2006)

traditional timber houses (*Joglo*). Most of the URM collapsed due to the lack of mechanical connection between roof, walls and floor. This structural failure was responsible for most of the deaths and injuries (Earthquake Engineering Research Institute (ERRI), 2006). In general, RM 1 and RM2 performed well during the 27 May 2006 earthquake, but several of them collapsed due to the poor connections between walls or columns and roof. Timber frame houses such as the Javanese traditional house or “*Joglo*” performed well because of their good connection between roof, columns, and floor. However, detailed investigation of 8 *Joglo* houses showed that 5 *Joglo* houses had collapsed while the rest of them were only slightly damaged. Based on thorough visual investigation, the damage of the *Joglo* houses can be classified into three main categories: columns-to leg connection; joint between main columns and beams; and roof construction and its attachment with the core structure (Prihatmaji et al. 2012).

The 27 May 2006 earthquake strongly impacted the Pleret Sub District in Bantul District, 10 km southeast of Yogyakarta city. Approximately 8,309 building units collapsed and 579 people died (BPS-Statistics of Bantul Regency 2010). After the reconstruction and rehabilitation processes finished, Pleret Sub District has been growing into one of the most densely populated areas in the southeast part of Yogyakarta City. The population of Pleret Sub District in 2013 was 45,136 people with a population growth rate of 0.05 (BPS-Statistics of Bantul Regency 2014). The increasing numbers of population in Pleret Sub District will also be followed by a rising demand for housing. As the population increases, the number of structures at risk also increases. Moreover, most of the buildings in Pleret Sub District are built on the top of dense volcanic sediment (Volcanic deposit of Merapi Volcano) which can amplify the earthquake wave and will increase the surface tremor when an earthquake occurs (Daryono, 2011). This condition increases the probability of a great disaster. Moreover, Java islands, especially in the south part of Java, often experience moderate to strong earthquakes ($M > 6.0$) with 50–100 years

of return period (Prihatmaji et al. 2012). Despite being experienced with the earthquakes, an integrated risk analysis of earthquake hazard for rural communities is still necessary in the research area. Therefore, the study of the comprehensive earthquake vulnerability of residential buildings based on the probabilistic model in geographic information systems (GIS) environment is needed in earthquake prone areas like Pleret Sub District. The buildings damage prediction can be obtained through the probabilistic analysis based on the building damage data of the 27 May 2006 earthquake. Additionally, GIS will provide a better explanation of building damage distribution in order to support the local government in disaster and risk management phase.

There was an immediate international response and reaction after the main shock at 05:54 local time at 27 May 2006. Approximately 100 response operations reacted quickly and brought to a rapid acquisition of satellite imagery to support the preliminary damage assessment process. A variety of damage maps were available in a week after the earthquake. Those damage maps mostly were produced by UN Institute for Training and Research (UNITAR)’s Operational Satellite Applications Programs (UNOSAT) (Kerle, 2010). The rapid ground survey was conducted by the Universitas Gadjah Mada (UGM) in Yogyakarta. As a result, an extensive database of building type, function and construction material of affected buildings were made available soon after the earthquake.

Probabilistic seismic hazard assessment (PSHA) and deterministic seismic hazard assessment (DSHA) have been growing rapidly both for governmental purposes and scientific research since the Yogyakarta earthquake in 2006. PSHA and DSHA help producing an earthquake hazard zonation in Yogyakarta and surrounding areas. However, the study about the damage patterns of Yogyakarta earthquake in research is limited and absolutely needed. A previous relevant study was conducted by Nurwihastuti, et al. (2014) which had the main objective to investigate the Yogyakarta damage pattern

through the geomorphological approach including investigation of surface and subsurface characteristics. The results showed that the most severe damage tended to occur in areas which had particular characteristics: a deep basement layer, low gravity anomaly, thick surface sediment, and unconsolidated surface material. Based on this result, a study about the relationship between building characteristics, site condition, and the damage level based on probabilistic analysis was regarded as important to give a complete understanding of earthquake damage pattern in Yogyakarta. The objectives of this study is to conduct a building vulnerability assessment based on probabilistic analysis and to estimate the vulnerability of buildings and population in the study area under different scenarios of population distribution.

Profile of study area

Pleret Sub District is located 10 km southeast of Yogyakarta City. It lies between 10° 22' 33" E - 110° 27' 00" E and between 7° 51' 12" S - 7° 54' 7" S. Pleret Sub District has a total area of 22.97 km², which consists of five villages: Wonolelo (4.54 km²), Bawuran (4.97 km²), Segoroyoso (4.87 km²), Pleret (4.25 km²), and Wonokromo (4.34 km²). Administratively, Pleret Sub District borders with other Sub district as follows:

- South boundary: Jetis Sub District and Imogiri Sub District
- East boundary: Dlingo Sub District
- North boundary: Banguntapan Sub District and Piyungan Sub District
- West boundary: Sewon Sub District and Jetis Sub District

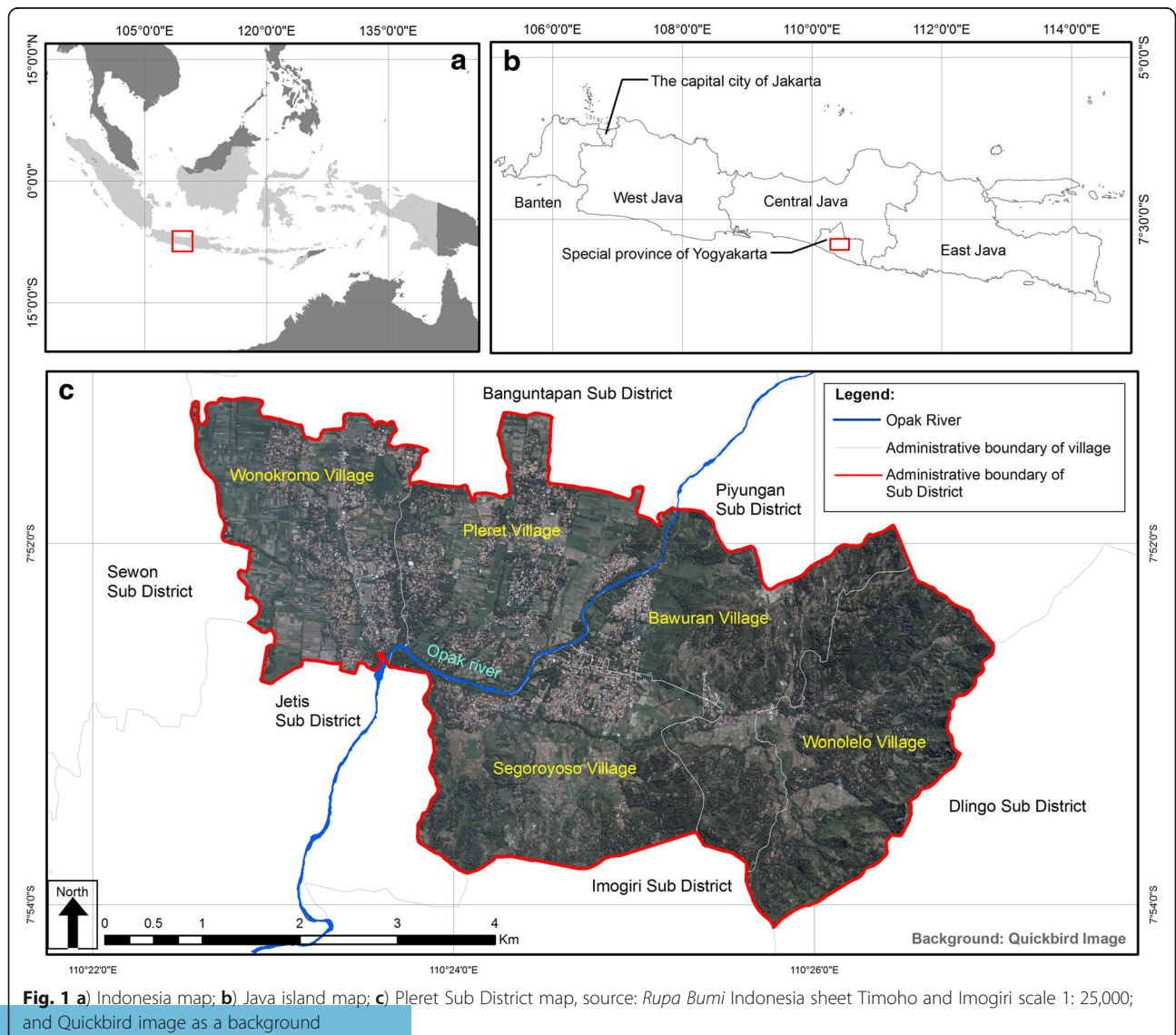


Fig. 1 a) Indonesia map; b) Java island map; c) Pleret Sub District map, source: *Rupa Bumi* Indonesia sheet Timoho and Imogiri scale 1: 25,000; and Quickbird image as a background

The Pleret Sub District map and the Quickbird satellite image showing the location of Pleret Sub District can be seen in the Fig. 1 below.

The Pleret Sub District is predominantly located on two major geological units. The main part of Pleret Sub District (the capital sub district) is situated in a low-relief alluvial deposit while the East area of Pleret consists of an ancient volcanic deposit which is collectively referred to as the Semilir Formation and Nglanggran Formation. According to the geological map of Yogyakarta (scale 1:100,000) (Rahardjo 1995), those two geological units can be subdivided into several smaller formation units as follows (see Fig. 2).

1. Alluvium (Qa):
it generally consists of gravel, sand, silt and clay along the river.
2. Young volcanic deposits of Merapi Volcano (Qmi):
it consists of undifferentiated tuff, ash, breccia, agglomerate and lava.
3. Nglanggran Formation (Tmn):
it is composed of volcanic breccia and lava flow containing breccia, agglomerate rock and tuff

4. Semilir Formation (Tmse):
it consists of interbedded tuff-breccia, pumice breccia, dacite tuff and andesite tuff and tuffaceous clay-stone.
Both the Nglanggran Formation (Tmn) and the Semilir Formation (Tmse) are the Tertiary volcanic deposits that were formed between late Oligocene and early Miocene, respectively (Mulyaningsih et al., 2011). Tmse consists of volcanic clastic materials with the pumice as the main material. This fragmental material has various grain size fragments starting from a very fine tuff until breccia pumice that has very coarse grains fragments (Yusliandi et al. 2013). The abundance of pumice fragments in Tmse indicates that Tmse is typically co-ignimbrite deposit. In term of volcanology sediment, the co-ignimbrite deposit can be classified as a volcanic material which was formed by close explosive eruption (Mulyaningsih et al., 2011); (Yusliandi et al. 2013); (Winarti 2015); (Bronto et al., 2009). On the contrary, Nglanggran Formation (Tmn) was formed as a result of an effusive eruption and deposited on the top of the Semilir Formation. Tmn consists of solid material of breccia, lava andesite, and basalt. This formation is wide-spread along the Baturagung Escarpment in the west part of Parangtritis and east part of Gunung Panggung. Similar to Semilir Formation, Nglanggran is

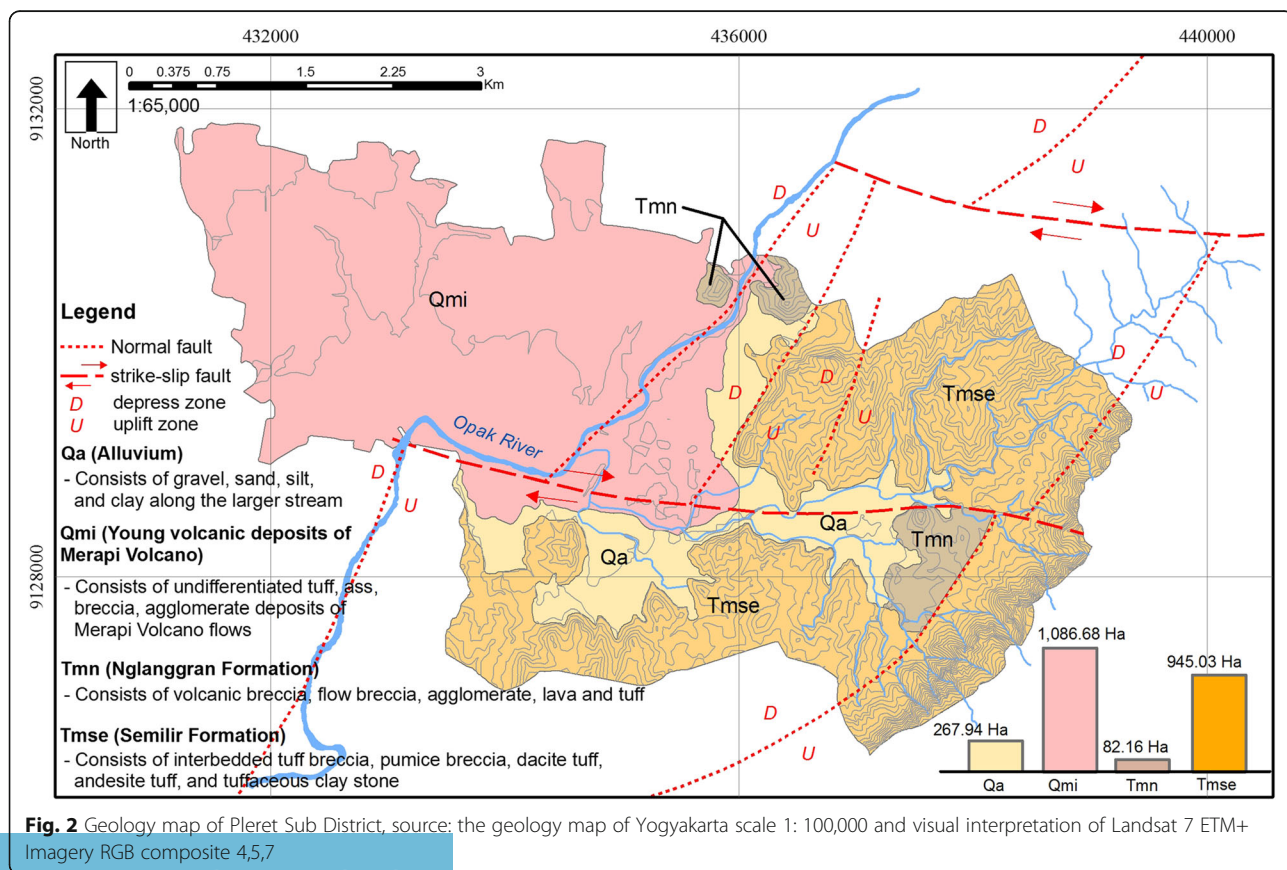


Fig. 2 Geology map of Pleret Sub District, source: the geology map of Yogyakarta scale 1: 100,000 and visual interpretation of Landsat 7 ETM+ Imagery RGB composite 4,5,7

lacking fossils. However, based on the foraminifera content that was found in the insertion of sandstone and claystone in the bottom-most layer, Nglanggran Formation is the middle Miocene deposits. These Miocene formations were buried by younger sedimentary rock including the Young Volcanic Deposits of Merapi Volcano (Qmi) and the Alluvium (Qa). The young volcanic deposits of Merapi Volcano consist of the Young Merapi Volcano sediment that was transported by several big rivers such as Opak River while the alluvium was formed through the denudation processes on the steep areas. The Qa and Qmi are characterized as dense soil located in the extensive flat land along the Opak River. In the eastern part of the research area, uplift and erosion have stripped away much of the cover rock, exposing the underlying rock, Nglanggran and Semilir Formation.

There are many geological faults formed in the research area, as a result of the plate movements along the subduction zone in the south part of the Java islands. One of them is known as Opak Fault which is often associated with the Opak River. Abidin, et al. (2009) concluded that this SW-NE normal fault is an active one. Another normal fault which has the same orientation with Opak Fault lies in the middle of the research area. This normal fault is known as Bawuran Fault. Both of

them have the same movement, i.e., the west part of the fault line is moving downward while the east part of the fault line is moving upward. There are also two major strikes-slip faults that located in the research area, namely Bawuran-Cinomati (centre part) and Becucu-Tekek Fault (north part) (see Fig. 2). Both of them were formed later after the development of Opak Fault. In the post-stage of uplifting movement of Opak Fault, the strike-slip faults were created and trimmed horizontally the research area into north and south area. The north part is moving eastward while the south part is moving westward (Sanjoto 2004).

Located on the western flank of Baturagung Escarpment, The Pleret Sub District has various topographical conditions. The lowest point (39.9 m) is located on the alluvial plain along the Opak River while the highest point (344.7 m) is located at the summit of Baturagung Escarpment. The steepest slopes (>350) are found at the hilly area of Baturagung Escarpment, located on the east side of the study area.

Based on their genesis, the general landform of Pleret Sub District consists of three major landforms of structural, fluvial and denudation origin. The structural landforms can be recognized from the morphological uplift and depress in the east and the west part of the study

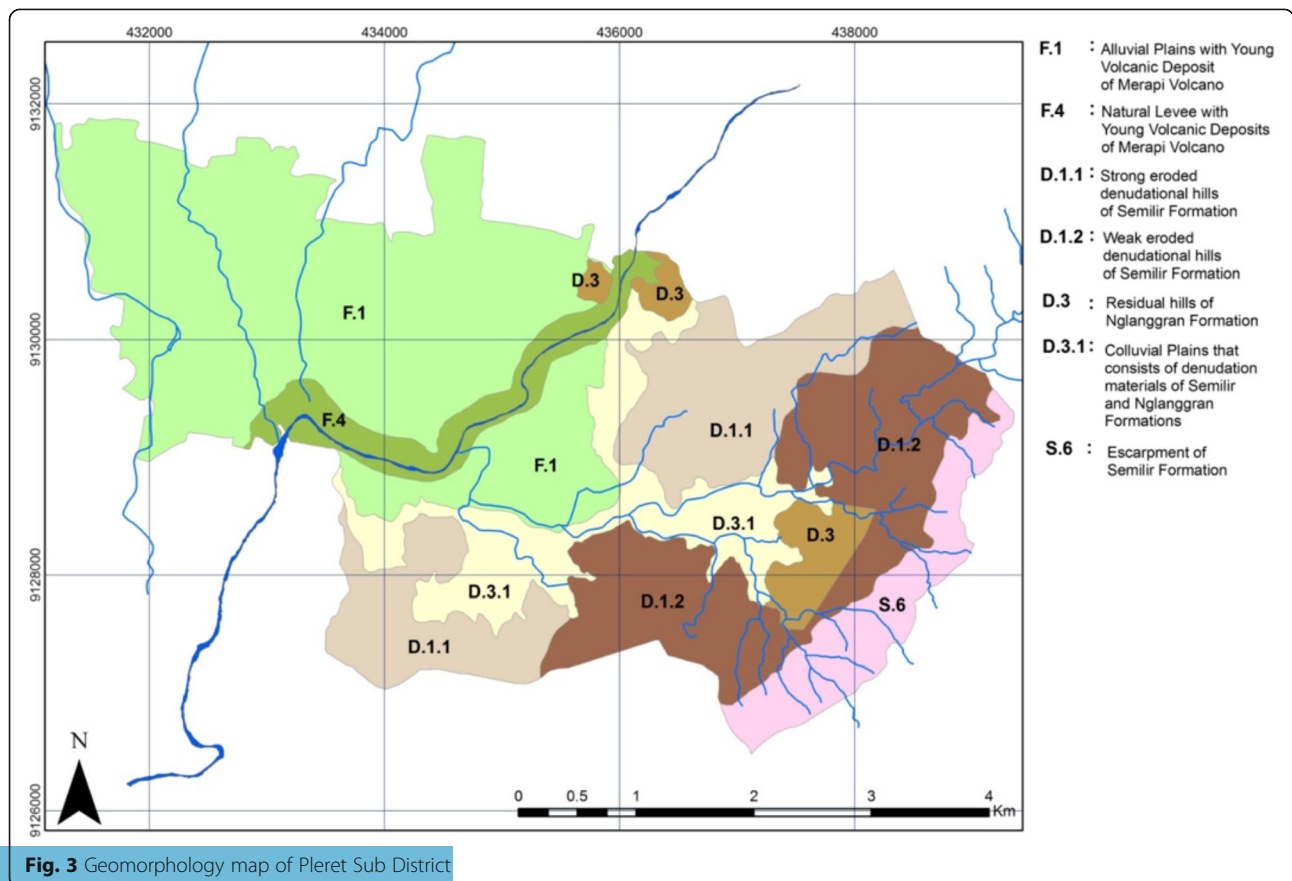


Fig. 3 Geomorphology map of Pleret Sub District

area. The intensive denudation processes occur in the middle and upper slope of the escarpment and the hilly area of Semilir Formation, which has less vegetation due to the intensive mining activities. The fluvial landform containing alluvial plain is located along the Opak River to the west part of study area including the main part of the Pleret Sub District (see Fig. 3)

Historical and recent earthquake events

Yogyakarta Province that lies in the south part of Java island is one of the most seismically active regions in Indonesia. This seismic condition is greatly influenced by the subduction process of the Indo-Australian and Eurasian Plates. Additionally, an active normal fault is also located in the middle part of the study area. This normal fault, Opak Fault, is associated with Opak River with SW-NE direction. The uplift zone is located to the east of this fault and vice versa. (Rahardjo et al. 1995).

Twelve great earthquakes between 1840 and 2006 were historically or instrumentally recorded near the Yogyakarta and Central Java Province. Many of these earthquakes caused damage, or even worse, casualties (Table 3). Based on the historical source, the 7.2 Mw earthquake with the epicentre offshore, 120 km SE of Yogyakarta City Centre, severely damaged 2,200 houses in 1937. Also, in 1943, an earthquake with the epicentre near the previous earthquake caused a death toll of 213 and destroyed 15,275 houses. One of the most recent strong earthquakes that caused several damages in Yogyakarta and Central Java Province including study area was on May 27, 2006, at 5:54 a.m. local time, with a moment magnitude of 6.4 which occurred 20 km SE of Yogyakarta City. The earthquake epicentre's as estimated by the United State Geological Survey (USGS) was 7.962°S – 110.458°E, and the focal depth was 10 km.

The tremors lasted for 52 s. The earthquake directly affected the Yogyakarta Province and Central Java area

The damage distribution was well correlated with the epicentre and presumed fault region. All regions nearby the Opak fault suffered a high death toll and massive damage including the study area. Walter et al. (2007) and Daryono (2011) concluded that damage pattern was highly controlled by the amplification factors. The earthquake amplification phenomena occurred in Young Merapi Volcanic Deposits which is located along the Opak River. This area was a densely populated area. Several sub districts that were within the amplification zone and had severe damage were Imogiri, Bambanglipuro, Jetis, Pleret, Banguntapan, Prambanan, Gantiwarno, Wedi and Bayat Sub Districts.

The collapsed buildings due to the ground shaking were mostly non-engineering buildings consisting of one or two storey houses, shops, religious and school buildings. Most of the collapsed residential buildings were non-engineering masonry houses. They were one storey tall with unreinforced clay, brick or block masonry in cement or lime mortar and no particular connection frame between timber roof and the walls. According to Elnashai, et al. (2006) these houses commonly had 8–20 m² of plan dimensions and 2.5 to 3 m of average heights. They usually used half brick masonry infill walls as a reinforced concrete framing. Damage was also found in reinforced masonry buildings. However, it was only moderate. The earthquake also affected several commercial buildings in the research area. Most of them suffered from slight damage until collapse. Those buildings were engineered multi-storey reinforced concrete structures (Elnashai et al., 2006). Examples of the building damages can be seen in Fig. 4 below

Table 3 Historic earthquakes data in Yogyakarta and Central Java Province

Date	Epicentre		Hypocentre (km)	Magnitude	Impact
	Latitude	Longitude			
04-01-1840	-	-	-	-	Followed by tsunami
20-10-1859	-	-	-	-	Followed by tsunami
10-06-1867	-	-	-	-	500 death tolls, thousands of houses damaged
28-03-1875	-	-	-	-	V-VII MMI scale
27-09-1937	8.88	110.65	-	7.2	VII-IX MMI; 2,200 of houses collapsed
23-07-1943	8.60	109.90	90	8.1	213 death tolls; 15,275 of houses damaged
12-10-1957	8.30	110.30	-	6.4	VI MMI scale
14-03-1981	7.20	109.30	33	6.0	VII MMI scale
09-06-1992	8.47	111.10	56	6.5	IV MMI scale
25-05-2001	8.62	110.10	50	6.2	IV MMI scale
19-08-2004	9.22	109.55	6.3	6.3	IV MMI scale
27-05-2006	7.96	110.45	15	6.4	more than 6,400 death tolls

Source: (Daryono, 2011)



Fig. 4 Buildings damaged types (Daryono, 2011)

An overview of existing building condition

The description of damaged buildings above may reveal that the buildings had been constructed with lack of anticipation on seismic events as well as quality of construction (Elnashai et al., 2006). Generally, buildings consist of non-structural and structural elements. Non-structural elements refer to the components of the building that are not considered to support its self-weight as well as the external forces of the building. On the other hand, the structural elements refer to the components of the building that are carefully designed to hold and distribute the forces acting on the building and transfer every single force to the ground continuously without any significant deformation. Each part of the structural elements of the building collaborates with each other to form a structural system that guarantees the utility of a building.

Rapid Visual Screening of Building for Potential Seismic Hazards (FEMA P-154) classifies building structure into 15 categories. Classification takes into account the combination between structural element material and structural load-bearing system. The building classification in this study is also in line with the FEMA P-154. Based on the previous research, (Aswandono, 2011 and Saputra, 2012), four categories of structure found in the study area, i.e.: URM - unreinforced masonry bearing-wall, W_1 - light wood-frame residential and commercial buildings smaller than or equal to 5,000 ft² ~ 460 m², RM_1 -reinforced masonry buildings with flexible floor and roof diaphragms, and RM_2 - reinforced masonry buildings with rigid floor and roof diaphragms (FEMA, 2015).

Within the URM building, the unreinforced fired clay brick masonry walls built in cement mortar act as the main load-bearing structure, while the wooden or bamboo roof as upper structure which also carries the load of clay tiles thereon. The upper structure is laid directly on the walls as the main structure with no special connection. This type of building works best in carrying gravity force, but it is very poor in resisting lateral forces. Consequently, URM building will experience severe damage or collapse under earthquakes' force (Wijanto &

Sinha, 2003). URM is generally categorized as a non-engineered construction which is built under the traditional construction practice on an empirical basis.

Light wood-frame buildings (W_1) in the study area are represented by traditional buildings which are the result of a long empirical process of trial and error in establishing a unique type structure (Prihatmaji et al. 2012). Traditional wood-frame structures were designed to deal with environmental threats to provide safety and convenience conditions for the people inside. The building is mainly built with wood which relatively results in significant reduction on the weight of building compared to that of different types of material. Since the seismic forces are proportional to the total weight of the building, the heavier building will suffer from greater horizontal force which might cause damage and even the collapse of the building. Another essential characteristic of light wood-frame structure is the common use of special connections which provide both strength and flexibility in responding forces. The connections will assure that the structural elements will be kept connected under a certain magnitude of forces and structural displacement in respond of the forces. Both light-weight and wooden connections provide structural flexibility to deal with seismic forces. However, the special characteristics of W_1 -type still do not guarantee that the building would be safe under an earthquake shake. According to Prihatmaji et al. (2012), there are three common damages causing the total of the Joglo Structure. First, the failure of the connection between the wood columns and the foundation due to the lacked of column-foundation especially in the side structure. Additionally, the column can easily slipped out from the bas stone when the column's leg decayed. Second, the failur of connection between lower and upper beam because the damage of both column and beam after receiving the lateral force of the earthquake. Third, the roof structure failure which is triggered by the detachment of the roof rafter from the main beam due to the deformation, unstable, or collpases of the outer structure.

Reinforced masonry buildings (RM) which use wood diaphragm and RM_2 which often use precast concrete

diaphragm, rely on the perimeter bearing wall to hold acting forces. Generally, reinforced masonry building types have relative stiffer structure which works well under moderate earthquake forces as far as the building code implementation and adequate construction practice and control are well executed (FEMA, 2015). However, the evidence of post-disaster building condition in the study area reveals that many buildings were not constructed to meet the requirement of earthquake-resistant building as regulated in several building code. The building cost is considered as the main problem for lower-income people at the study area. A considerable number of buildings were constructed under poor construction practice by low-cost, incompetent traditional builders, without compliance with any safety rules and regulations and sufficient knowledge in construction science and earthquake engineering. In addition, the choice of low-quality material also significantly contributes to the poor building quality.

Demographic condition

According to the civil registration data of Bantul District, the population of Pleret Sub District in 2013 was 45,316 people with an average population growth of 1.99%. The sex ratio of Pleret Sub District was 100.34, which means that the numbers of females and males in the population are relatively balanced. Wonokromo and Pleret Villages are the densest areas in Pleret Sub District with the population density being 3,231 and 2,953 people per km² respectively. Whereas, the lowest population density (1,003 people per km²) is Wonolelo Village, which is located in the eastern part of Pleret. The demographic structure in this sub district displays a near-stationary pyramid. The 2013 demographic data showed that this area has stable growth and was dominated by productive people between 15 and 49 years of age. This age group is relatively less vulnerable than the other ones. On the other hand, approximately 43% of

the total population in Pleret Sub District is more susceptible to earthquake casualties due to their ages (>14 and < 49 years old) (Fig. 5).

Based on the latest uploaded data (Wonokromo Village, 2014; Pleret Village, 2014; Segoroyoso Village, 2014; Bawuran Village, 2014; and Wonolelo Village 2014), there are five major types of occupation in Pleret Sub District, i.e., the casual worker, student, unemployment, entrepreneur and farm worker. Almost 20% of the total population in Pleret Sub District are casual workers, 13.55% are students, 13.39% work as entrepreneurs, 11.37% are farm workers, and 13.10% are unemployed. The detail of occupation types in Pleret Sub District can be seen in Table 4. This type of data, i.e. type of population occupation of each village, are imperative in vulnerability studies especially for modelling human vulnerability based on spatiotemporal distribution (Freire et al. 2013).

Method

Three main analyses were applied in this study; first, the visual interpretation of geological features and land use; second, the probabilistic analysis of building damage; and third, the population distribution analysis. The Landsat 7 ETM+ and Quickbird 2012 satellite imagery were utilized to generate the geology and land use map in the areas of interest. The probabilistic analysis was done by using the building damage dataset which is obtained from the rapid survey of earthquake damage after the Yogyakarta earthquake, 2006. In addition, to disaggregate the numbers of population into particular land use units, this study used the data of local livelihood obtained from the local government at village level. The final results of this study is the multi vulnerability model which was combination between the damage probability of building block and the population distribution model. The multi-vulnerability model was visualised in a map form with the scale of 1: 30,000.

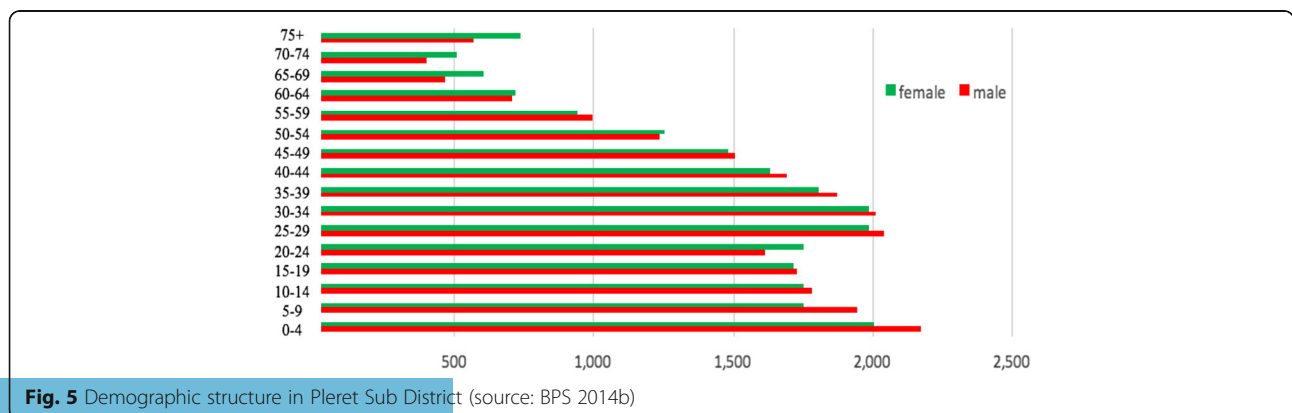


Fig. 5 Demographic structure in Pleret Sub District (source: BPS 2014b)

Table 4 Type of occupation of Pleret dweller

No	Type of occupation	Wonokromo (%)	Pleret (%)	Segoroyoso (%)	Bawuran (%)	Wonolelo (%)
1	casual Worker	17.92	20.51	18.86	20.16	23.99
2	student	16.03	13.89	12.60	11.55	9.89
3	unemployed	13.69	12.89	12.88	13.32	12.11
4	entrepreneur	11.84	12.88	16.72	16.12	9.55
5	farm worker	8.86	11.03	12.17	13.59	15.18
6	private employee	6.74	5.31	2.85	3.59	2.75
7	housewife	5.42	3.71	2.58	3.27	1.78
8	government employee	2.77	2.06	1.14	0.76	1.20
9	retired	1.24	0.93	0.47	0.35	0.82
10	trader	0.60	0.94	1.95	1.41	0.68
11	teacher	0.50	0.55	0.31	0.33	0.23
12	police officer	0.31	0.32	0.24	0.23	0.13
13	farmer	0.25	0.23	0.96	0.90	2.77
14	Army	0.21	0.27	0.13	0.08	0.13
15	honorary employee	0.13	0.10	0.13	0.08	0.04
16	village official	0.12	0.11	0.13	0.23	0.27
17	rock miner	0.08	0.02	0.06	0.05	0.00
18	state-owned enterprise	0.07	0.05	0.02	0.03	0.02
19	religious teacher ("ustadz")	0.07	0.01	0.02	0.03	0.04
20	driver	0.08	0.09	0.09	0.07	0.08
21	dress maker	0.05	0.15	0.09	0.18	0.02
22	lecturer	0.05	0.09	0.03	0.02	0.02
23	nurse	0.05	0.06	0.01	0.00	0.02
24	doctor	0.04	0.02	0.05	0.02	0.00
25	midwife	0.03	0.00	0.00	0.05	0.02
26	housemaid	0.03	0.02	0.02	0.03	0.00
27	lawyer	0.02	0.01	0.00	0.00	0.00
28	reporter	0.02	0.01	0.00	0.00	0.00
29	regional owned enterprise	0.02	0.00	0.00	0.02	0.00
30	carpenter	0.04	0.01	0.02	0.66	0.17
31	mechanic	0.01	0.02	0.02	0.03	0.00
32	consultant	0.01	0.00	0.00	0.00	0.00
33	electrician	0.01	0.00	0.00	0.00	0.00
34	breeder	0.01	0.01	0.01	0.00	0.02
35	artist	0.01	0.02	0.01	0.00	0.02
36	make up man	0.01	0.00	0.01	0.00	0.00
37	headman	0.01	0.01	0.01	0.02	0.00
38	traditional healer	0.00	0.01	0.00	0.02	0.00
39	chief	0.00	0.01	0.00	0.00	0.00
40	pharmacist	0.00	0.01	0.00	0.00	0.00
41	sailor	0.00	0.01	0.00	0.00	0.00
42	provincial council member	0.00	0.00	0.01	0.00	0.00
43	other (no data)	12.65	13.65	15.39	12.81	18.03

Source: (Wonokromo Village, 2014) (Pleret Village, 2014) (Segoroyoso Village, 2014) (Bawuran Village, 2014) (Wonolelo Village 2014)

Visual interpretation

A series of visual interpretation elements such as colour/tone, size, shape, texture, pattern, shadow, and association were used to distinguish the types of land use and the geological features. The first stage is the land use data extraction through the visual interpretation of Quickbird imagery. The USGS land use and land cover classification system was used to divide the land use into several major groups. Those major groups are urban or built-up land; agricultural land; rangeland; forestland; water; wetlands; barren land; and managed wetland. The main difficulties of land use interpretation in the research area are to differentiate the residential and non-residential buildings such as schools, hospitals, governmental offices, mosques, light industrial buildings, and traditional markets. The residential buildings usually have a regular shape (rectangle) and the building size lies between 21 m² and 200 m². The school buildings have irregular shapes (e.g. shape of letter "O", "L", "U", "T", and "H") and are mostly located near playgrounds or open areas. The governmental offices and hospitals are usually comprised of several smaller building units with regular shapes, close to each other, and have the same colour of roof material. Light industrial buildings and traditional markets usually have a large building size (>200 m²) and they use asbestos or zinc roofs which is indicated by the white or grey roof colour in Quickbird Imagery. The mosques in the research area have a specific roof shape ("*limasan*"), and are located near the public cemetery (Fig. 10). The commercial strip development refers to the commercial activity developed along the main road such as shops, retail stores, fast food services, gas stations, etc. In general, the commercial strip has the same characteristics as the residential buildings. The key criterion to differentiate the commercial strip from the settlement is the proximity to the main road. Most shops, retail stores, fast food services and other similar goods and services are located along the main road and vehicular transportation road.

The next step is to identify the geological characteristics through visual interpretation of Landsat 7 ETM+. The visual interpretation elements of colour/tone, shape, pattern, texture, and association were used to extract the geological information. Moreover, a 1: 100,000 geology map of Yogyakarta and a topographic map with a 12.5 m contour interval were also used to support the interpretation process. The geological features were obtained from the visual interpretation process of Landsat 7 ETM + imagery with RGB colour composite of 4,5,7. The Band 4 or near infrared (0.7-0.9µm) is good for determining water or land surfaces because almost all radiation in this wavelength range is absorbed by water. The band 5 or middle infrared (1.55-1.75 µm) is very sensitive to moisture and very suitable to monitor vegetation.

The band 7 or middle infrared (2.08-2.35 µm) is good for soil and geological mapping. By using the elements of interpretation and topographic information such as relief and slope, a detailed unit of geological unit can be produced to complement the geology map. Finally, a fieldwork has been conducted to justify qualitatively the accuracy of geological interpretation. At least 53 observation locations have been identified and verified in term of the geological unit characteristic. A physical characteristic identification of the outcrops or surface sediment have been conducted in the field. The rock and formation classification referred to the Geological map of Yogyakarta scale 1: 100,000.

Probabilistic analysis of building damage

A statistical analysis was applied to calculate the probability of building damage based on the damage building inventory data. An ordinal logistic regression was used to generate a probabilistic model of building damages. This modelling method was used because the dependent variable (damage level) is a 3-level ordinal data. The number "1" means not damaged, 2 is moderately damaged, and 3 is collapsed. These damage levels were obtained from rapid damage assessment after the Yogyakarta earthquake 2006 (Kerle, 2010). The independent variables were the structure types (reinforced masonry, unreinforced masonry, and wood); roof material (asbestos or zinc, cement tile, clay tile, concrete slab, and thatch); distance (within 8 km, 8.1–10 km, 10.1–12 km, and 12.1–15 km); geology (Qa, Qmi, Tmn, and Tmse). However, because of the low frequency, thatch roof variable was taken out from the analysis. The summary of data used in the statistical analysis is provided in Table 5 below.

Before running the above ordinal logistic regression model in SPSS software, a benchmark or base value was defined for each variable (Leech et al. 2005). The building structure in this case is represented by three variables namely Structure = 0; Structure = 1; and Structure = 2. It is necessary to define one variable to be a base value among those three variables in order to help with the interpretation of the results. Reinforced masonry (Structure = 2) is defined as the base value for variable 1 and 2. Roof = 3 is defined as the base value for variables 4, 5, and 6. Distance = 4 is defined as the base value for variables 8, 9, and 10 and the last benchmark is Geology = 3 for variables 12, 13, and 14. The last step was to implement the probabilistic model into the 2012 building foot print data and to model the spatio-temporal patterns of residential building damage. A dasymetric mapping was applied in this model to disaggregate the numbers of population in space and time. The summary of the data used in this study can be seen in the Table 6 below.

Table 5 Variable used in statistical analysis

No	Variable	Type data	value	Other name
Dependent variable (Y)				
1	Building damage	Ordinal		Damage
	- Not damaged		1	
	- Moderately damaged		2	
	- Collapsed		3	
Independent variable (X)				
1	Wood structure	Binary	(0 or 1)	Structure = 0
2	Unreinforced masonry	Binary	(0 or 1)	Structure = 1
3	Reinforced masonry	Binary	(0 or 1)	Structure = 2
4	Asbestos or zinc roof	Binary	(0 or 1)	Roof = 0
5	Cement tile roof	Binary	(0 or 1)	Roof = 1
6	Clay tile roof	Binary	(0 or 1)	Roof = 2
7	Concrete slap roof	Binary	(0 or 1)	Roof = 3
8	Within 8 km from the epicentre	Binary	(0 or 1)	Distance = 1
9	Between 8.1–10 km	Binary	(0 or 1)	Distance = 2
10	Between 10.1–12 km	Binary	(0 or 1)	Distance = 3
11	Between 12.1–15 km	Binary	(0 or 1)	Distance = 4
12	Semilir Formation (Tmse)	Binary	(0 or 1)	Geology = 0
13	Alluvium (Qa)	Binary	(0 or 1)	Geology = 1
14	Young Merapi Volcanic deposit (Qmi)	Binary	(0 or 1)	Geology = 2
15	Nglanggran Formation (Tmn)	Binary	(0 or 1)	Geology = 3

Population distribution analysis

The population distribution in this study refers to the population distribution based on the community habits during the weekdays and holidays. The basic technique used was dasymetric mapping. The land use and the type of occupation were used to increase the accuracy of population distribution model. The adopted concept of dasymetric mapping can be seen in the Fig. 6 below.

The dasymetric model was conducted in several steps; first, the land use data was divided into binary values of population distribution (non-populated area

and populated area). Second, the population density of each land use unit was estimated. Third, a dynamic population distribution based on the community habits was made. The latter is very important, because human distribution in space varies largely during daily life (Freire et al. 2013).

Several equations are used to disaggregate the numbers of population

$$Xd = \sum_{i=1}^n Pi \tag{1}$$

Table 6 The main data used

No	Data	Data type	Obtained from	Function
1	Building footprint	Shape file (.shp), polygon	Visual interpretation of Quickbird Imagery 2012	Generate building the vulnerability map
2	Building damage data	Shape file (.shp), point	Preliminary damage assessment conducted by Gadjah Mada University	Generate probabilistic model through statistical analysis
3	Geologic data	Shape file (.shp) Polygon	Improve the geological map with visual interpretation results of LANDSAT 7 ETM+	Generate the building vulnerability map
4	Population characteristic	report	Pleret in Figure, 2014 Published by BPS-Statistic of Bantul Regency	Generate the temporal modelling of population distribution
5	Land use data	Shape file (.shp) polygon	Visual interpretation of Quickbird imagery 2012	Generate the dasymetric map

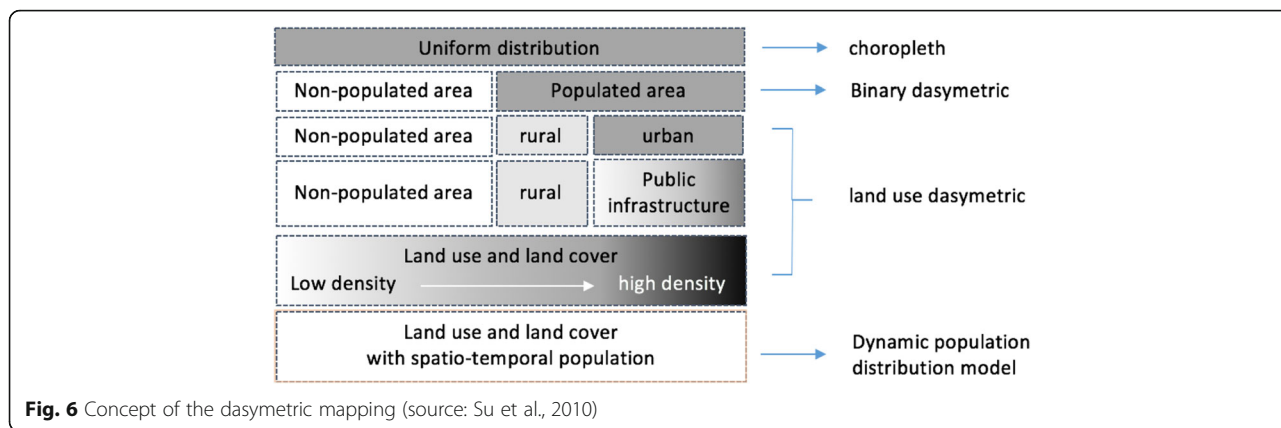


Fig. 6 Concept of the dasymetric mapping (source: Su et al., 2010)

$$P_i = \sum_{j=1}^n P_{ij} \tag{2}$$

$$P_{ij} = \frac{S_{ij}}{\sum_{i,j=1}^n S_{ij}} \cdot W_i \cdot X_d \tag{3}$$

Where:

- X_d = Number of people in administrative unit
- P_i = Number of people in land use i
- P_{ij} = Number of people in polygon j in land use i
- S_{ij} = Size polygon j in land use i in administrative unit
- W_i = Weight of land use i ,

The general framework of the research can be seen in Fig. 7 below.

Minimum, maximum, and average scenarios

In order to generalize the building damage probability value at building blocks level, three scenarios (minimum, maximum, and average scenarios) of building damage probability were applied. The illustration of converting the damage probability of each building unit into the damage probability of building block can be seen in the Fig. 7.

The predicted damage category of each building unit was calculated using the equation resulted from the

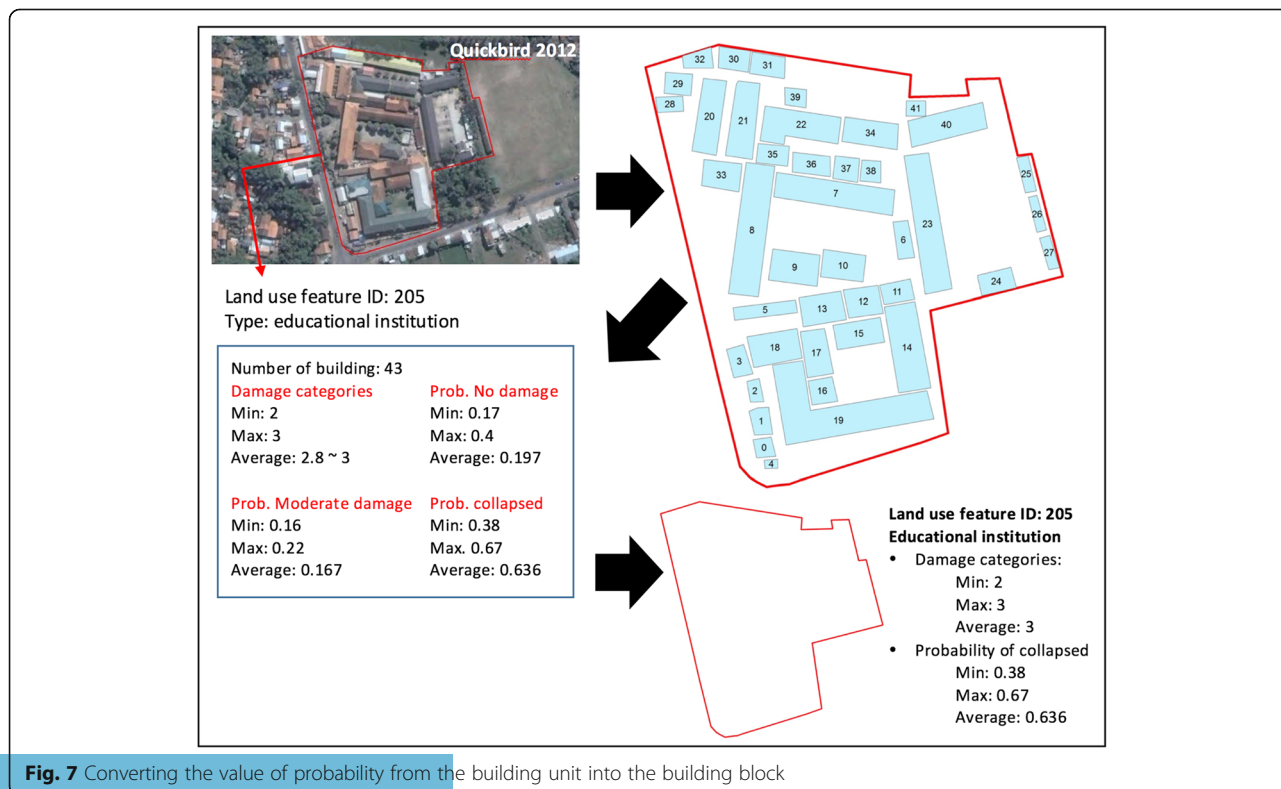


Fig. 7 Converting the value of probability from the building unit into the building block

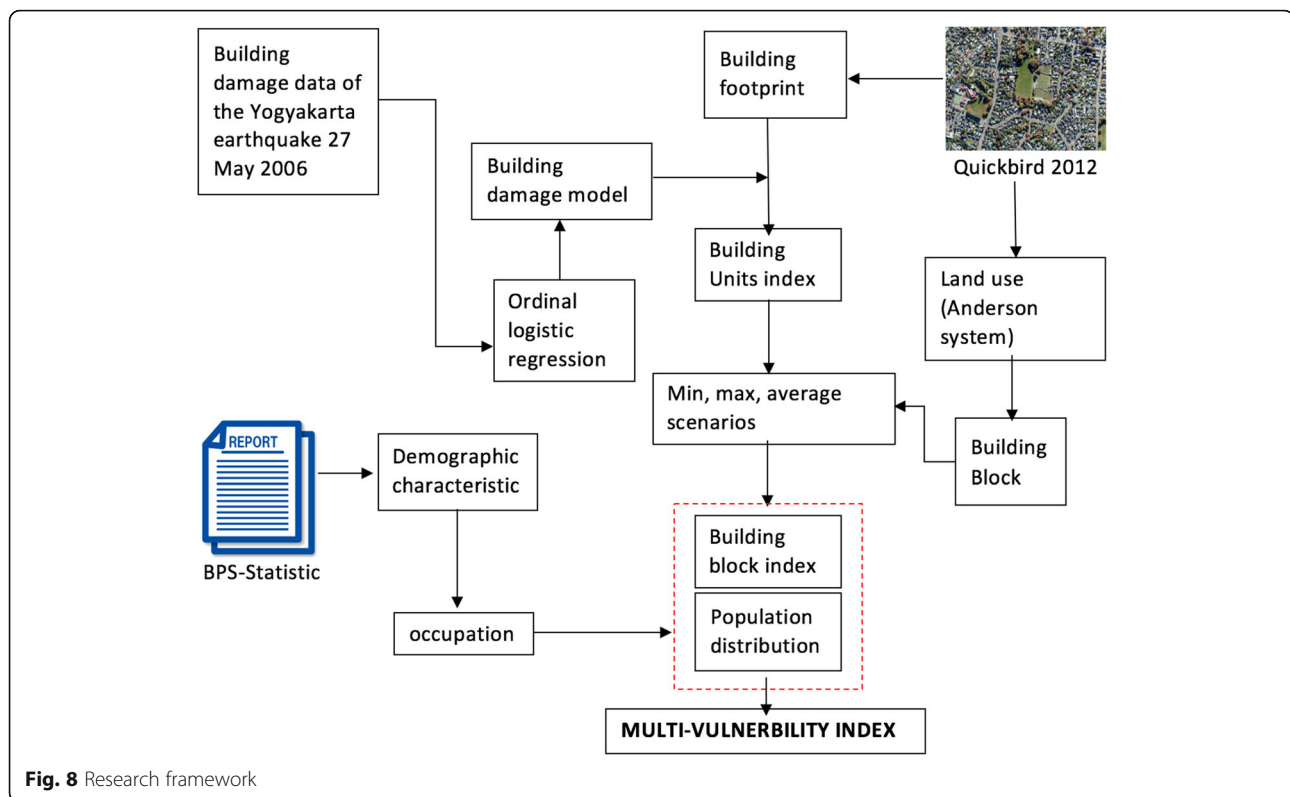


Fig. 8 Research framework

ordinal logistic regression (equation 4). Afterwards, the probabilities of not damaged, moderately damaged, and collapse were calculated using the equations 5, 6, and 7). Then, the separation of building land use from the others was done with the “select by attribute” tools in ArcGis 9.0. Based on the modified Anderson system 2002 (U.S. Geological Survey, 2007), the building land use consists of commercial strip development, educational institution, government centre, hospital, light industrial, mosque, residential area (high, medium, and low density), rural, single unit residential, and traditional market.

Estimating multi-vulnerability (Building damage category and population distribution)

The multi-vulnerability of buildings was determined by adding the building damage category (average scenario) and population distribution class. There are three classes of the numbers of population staying in the particular land use units. Class 1 refers to numbers of population below 100 people, class 2 to numbers of population between 100 and 200 people, and class 3 to numbers of population above 200 people. This classification follows the rule of natural break technique in GIS reclassify tools. The multi-vulnerability value will range between 2 and 6. The values of 2 and 3 are defined as low vulnerability, the value of 3 and 5–6 as medium and high vulnerabilities, respectively. The overall research framework can be seen in the Fig. 8 below.

Results

Visual interpretation of Landsat 7 ETM+ imagery to improve geological map of research area

Based on the visual interpretation of Landsat 7 ETM+, the research area was classified into four geological units. These units have unique characteristic of colour and tone, relief, and texture. Those geological units are Semilir Formation (Tmse), Nglanggran Formation (Tmn), Alluvium (Qa), and Young Merapi Volcano deposit (Qmi). The total area of Tmse in east part of Pleret Sub District is about 945.03 Ha (39.67%). Tmse is characterized with the domination of light blue colour and some random of reddish brown spot. Tmse has very rough texture, especially in the east part area, and is located between undulating slope and step slope areas ($4^{\circ} < \text{slope} < 35^{\circ}$). Different from Tmse, Tmn has a striking red colour with a few random of light blue spots. This unit is located in the eastern part of the research area and most of Tmn is in the flat area with the highest elevation being 334.7 m above sea level. This area extends to approximate 82.16 Ha. Qa and Qmi are very difficult to distinguish in the interpretation process, because both of them have similar characteristics of morphology, colour or tone, texture, and relief. Therefore, the field investigation was conducted to distinguish both geological units and to check the visual interpretation results.

There are some fundamental differences between the geological units derived from visual interpretation and the 1:100,000 geological map of Yogyakarta. Based on the latter, the border between Tmse and Tmn is located along the foot slope of Baturagung Escarpment near the Guyangan Villages, but we found that the border is located in the upper slope of Baturagung Escarpment near the Dlingo Villages. Then, we also found that there are some isolated hills in the north part of research area which is belong to the Tmn units. The main difference was also found in the extents of Qmi. Based on the visual interpretation, Qmi is spread along the left and the right side of Opak River, while the alluvium only occupies the small part of flat area near the hilly area of Semilir Formation. The summary of interpretation results and the differences between both geological maps are shown in Table 7 and Fig. 9.

The rapid field identification was conducted to determine the border between Qmi and Qa. Two approaches were used to determine both geological units. The first approach was to locate the boulder location. Qmi is dominated by fluvial process and produces very well sorted sediment. The upper layer consists of very fine sediment, while the lower layer consists of rough sediment. The boulder indicate that the particular area is influenced by the colluvium sediment which is characterized as bad sorted or mixture sediment from the hilly area nearby. The second approach is the clay content of both Qmi and Qa. Qmi tends to have less clay content being the Merapi Volcano sediment, while the Qa tends to have more clay content as it is the denudation material of the weathering process in the hilly surrounding areas. Therefore, one of the objectives of the rapid field investigation was to locate the traditional brick factory along the Opak River. The brick makers tend to use the

best soil which has less clay rather than soil which has more clay. The reason is that the brick will crack during the heating process if there are a lot of clay contents inside the soil. Therefore, the location of traditional brick makers can be used to indicate the Qmi area.

Based on the field observation and investigation, the geological unit's characteristic in the field is 100% the same as the information given in the improved geological map of the research area. The field documentation of rapid field investigation, is shown in Fig. 10.


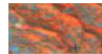


Land use interpretation

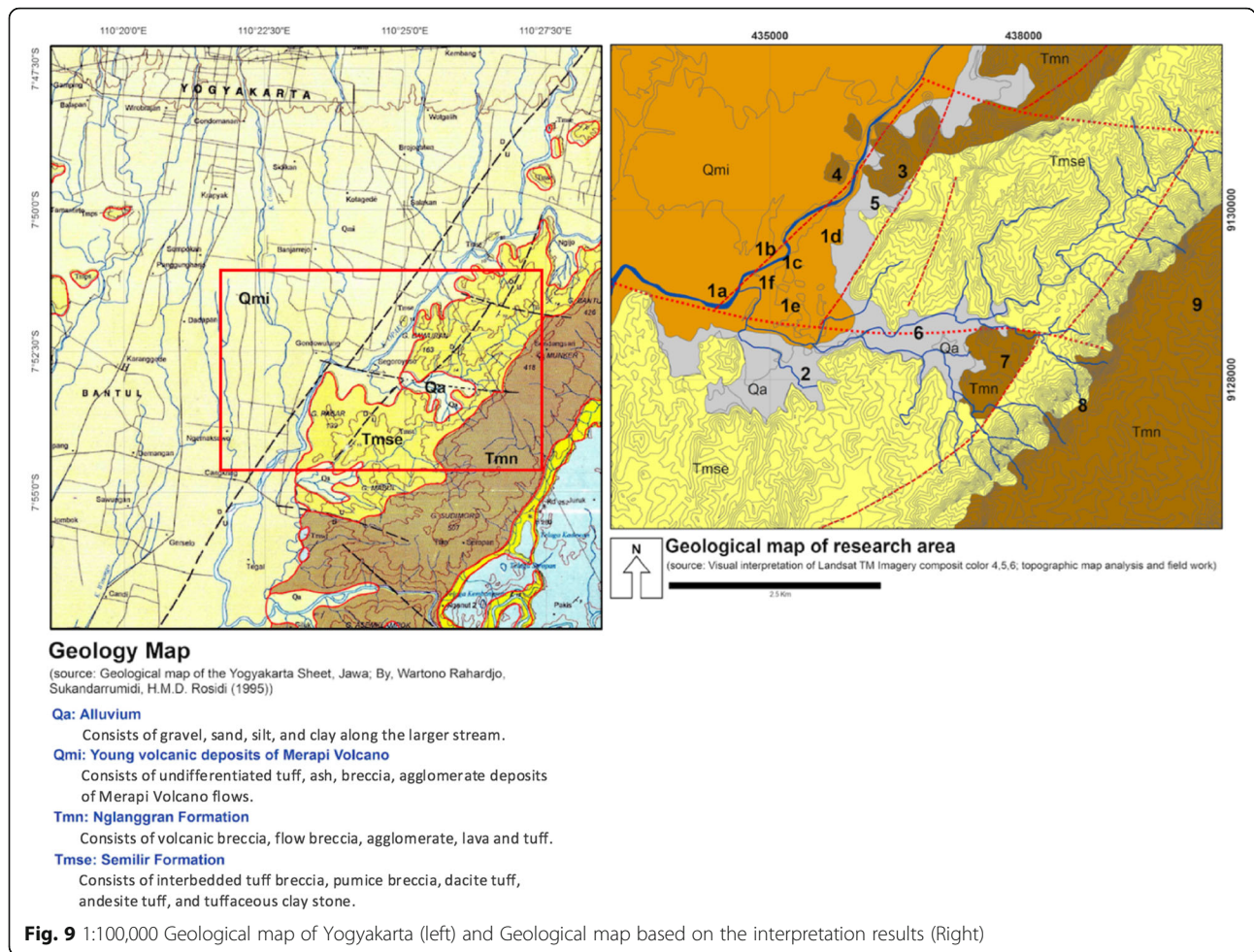
Based on the Land use- Land cover classification system, NJDEP modified Anderson System 2002, there are 29 land use units in the research areas. Those land use units cover 10 units of level 1 i.e., residential, commercial, industrial, transportation, other built up area, agricultural area, confined feeding operation, forestland, stream & canal, and wetland. The land use classification show that the research area is dominated by the shrub land which cover approximately of 42.36% of the total area. The wetland agricultural area or paddy field only cover 25.34% of the total area, while the residential area (high, medium, and low density) cover approximately 3.79%, 5.70% and 3.01%, respectively. Most of them are distributed in the west and middle part of research area which are the Qmi and Qa. Detail information is shown in Fig. 11, and Table 8, while the land use map is shown in Fig. 12.

Statistical results

The main objective of using statistical analysis in this study was to derive a model showing the relationship between the level of damage in residential houses and their characteristics. This study applied the ordinal logistic

Table 7 The characteristic of each geological unit resulted by visual interpretation using Landsat 7 ETM+

Geological unit	Colour or tone	Texture	Relief	Landsat 7 ETM+
Tmse	Light blue with random reddish brown spots	Very rough	Undulating to hilly areas	
Tmn	Red with random light blue colour	Rough	Flat area	
Qa	Combination of blue and red colour	Very fine	Flat area	
Qmi	Combination of blue and red colour	Very fine	Flat area	



regression because the dependent variable is a discrete ordinal data. The results show that the model is significant and can be used to the next level of analysis (Table 9), explaining approximately 33.20% of variance (Nagelkerke Pseudo R-square) (Table 10). After logistic regression analysis with 11 independent variables (without benchmark), the parameter estimates table was obtained (Table 11). This table gives information about the relationship of all independent variables with their benchmarks. For example, wood structure (-0.255) is better than the reinforced masonry structure, while the unreinforced masonry gives the worse result (0.685) compared to the reinforced masonry. In terms of roof material, concrete slab is the best roof type considering its low probability of collapsing. Tmse is better than the benchmark (-1.413), while the Qmi gives the worse results (1.507) comparing with the Tmn. This result fits very well with the real condition of building damage patterns caused by the 2006 Yogyakarta Earthquake. The most severe damage occurred in Qmi, which has lower value of local gravity, deeper basement, thicker sediment,

unconsolidated sediment, and unconsolidated material (Nurwihastuti et al., 2014).

Based on the Table 11, there are three categories of predicted response value namely, Y1, Y2 and Y3. Y1 refers to the not damaged category, Y2 refers to the moderately damaged category, and Y3 refers to the collapsed category. These categories were determined based on the threshold value in Table 11. Therefore, the predicted response values are defined as follow.

- $Y_i = Y_1$ if $Y^*_i \leq 1.529$ (Threshold Damage = 1)
- $Y_i = Y_2$ if $1.529 < Y^*_i < 2.426$ (Threshold Damage = 2)
- $Y_i = Y_3$ if $Y^*_i \geq 2.426$

The Y^*_i value can be calculated by applying the regression equation (equation 4) to the dataset of building footprint. There are 17,512 data of building units with 33 combination of building structure, roof material, distance from the epicentre, and the geological type. The example of the calculation can be seen in Table 12.



Fig. 10 The documentation of field verification



Fig. 11 Land use identification through visual interpretation of Quickbird

Table 8 The land use categories of Pleret Sub District

No	Land use	Area (Ha)
1	Abandoned mining sites	0.40
2	Agricultural wetlands	603.42
3	Canal	5.81
4	Cemetery	2.57
5	Cemetery on wetland	1.76
6	Commercial strip development	16.02
7	Educational institutions	11.42
8	Government centres	3.43
9	Harvested cropland	13.27
10	Health institution	0.61
11	Inactive cropland	5.02
12	Light industrial	3.00
13	Not built up	9.57
14	Open areas	14.30
15	Other agricultural	162.98
16	Other institutional (Mosque)	2.35
17	Pastureland	61.69
18	Poultry farm	1.95
19	Residential high density	90.16
20	Residential medium density	135.79
21	Residential low density	71.78
22	Road	64.61
23	Rural single unit	47.78
24	Shrub land	1,008.86
25	Specialty farm	3.68
26	Stone quarries	12.42
27	Stream	24.91
28	Traditional Market	1.42
29	Wetlands	0.71

$$\begin{aligned}
 Y * i = & -0.255 \text{ (wood structure)} + 0.685 \text{ (unreinforced masonry)} \\
 & + 0 \text{ (reinforced masonry)} + 0.43 \text{ (asbestos or zinc roof)} \\
 & + 0.749 \text{ (cement tile roof)} + 1.634 \text{ (clay tile roof)} \\
 & + 0 \text{ (concrete slab roof)} \\
 & + 2.265 \text{ (within 8km from the 2006 earthquake)} \\
 & + 0.949 \text{ (between 8.1-10 km)} + 0.744 \text{ (between 10.1-12 km)} \\
 & + 0 \text{ (> 12 km)} - 1.413 \text{ (Semilir Formation, Tmse)} \\
 & - 0.64 \text{ (Alluvium, Qa)} \\
 & + 1.507 \text{ (Young Merapi Volcanic Deposit, Qmi)} \\
 & + 0 \text{ (Nglanggran Formation, Tmn)}
 \end{aligned}
 \tag{4}$$

Based on the Table 12, specific combinations of building attributes (structure, roof, distance, and geology) give a particular damage category (Y*i value). For instance, combination 1 has 22 buildings with the same combination, i.e., wood structure, reinforced

masonry structure, located between 8.1 and 10 km from the epicentre, and located in Semilir Formation. This combination gives a value of Y*i equal to 0.915 which means that this building tends to have a low level of damage or not damaged. The probability of collapse can be also calculated by put the Y*i into general equation of ordinal logistic regression. The probability of damage of building attribute number 1 is as follows:

– Not damaged probabilistic (Y1)

$$Y1 = 1 / (1 + e^{(Y * i - \text{threshold} 1)}) \tag{5}$$

– Moderately damaged probabilistic (Y2)

$$Y2 = 1 / (1 + e^{(Y * i - \text{threshold} 2)}) - Y1 = 1 / (1 + e^{(Y * i - \text{threshold} 1)}) \tag{6}$$

– Collapsed probability (Y3)

$$Y3 = 1 - 1 / (1 + e^{(Y * i - \text{threshold} 2)}) \tag{7}$$

Therefore,

$$Y1 = 1 / (1 + e^{(Y * i - \text{threshold} 1)})$$

$$Y1 = 1 / (1 + 2.718^{(0.915 - 1.529)})$$

$$Y1 = 1 / (1 + 2.718^{(-0.614)})$$

$$Y1 = 1 / (1 + 0.541216)$$

$$Y1 = 1 / 1.541216$$

$$Y1 = 0.64884 \text{ (Probability of not damaged)}$$

$$Y2 = 1 / (1 + e^{(Y * i - \text{threshold} 2)}) - Y1 = 1 / (1 + e^{(Y * i - \text{threshold} 1)})$$

$$Y2 = 1 / (1 + 2.718^{(0.915 - 2.426)}) - 0.64884$$

$$Y2 = 1 / (1 + 2.718^{(-1.511)}) - 0.64884$$

$$Y2 = 1 / (1 + 0.2272) - 0.64884$$

$$Y2 = 1 / 1.2272 - 0.64884$$

$$Y2 = 0.81919 - 0.64884$$

$$Y2 = 0.17035 \text{ (Probability of moderately damaged)}$$

$$Y3 = 1 - 1 / (1 + e^{(Y * i - \text{threshold} 2)})$$

$$Y3 = 1 - 0.81919$$

$$Y3 = 0.18081 \text{ (Probability of collapsed)}$$

Table 13 shows the complete results of probability calculation of 33 buildings attribute combination in research area. Based on the calculation of building damage probability, the safest building type is the combination

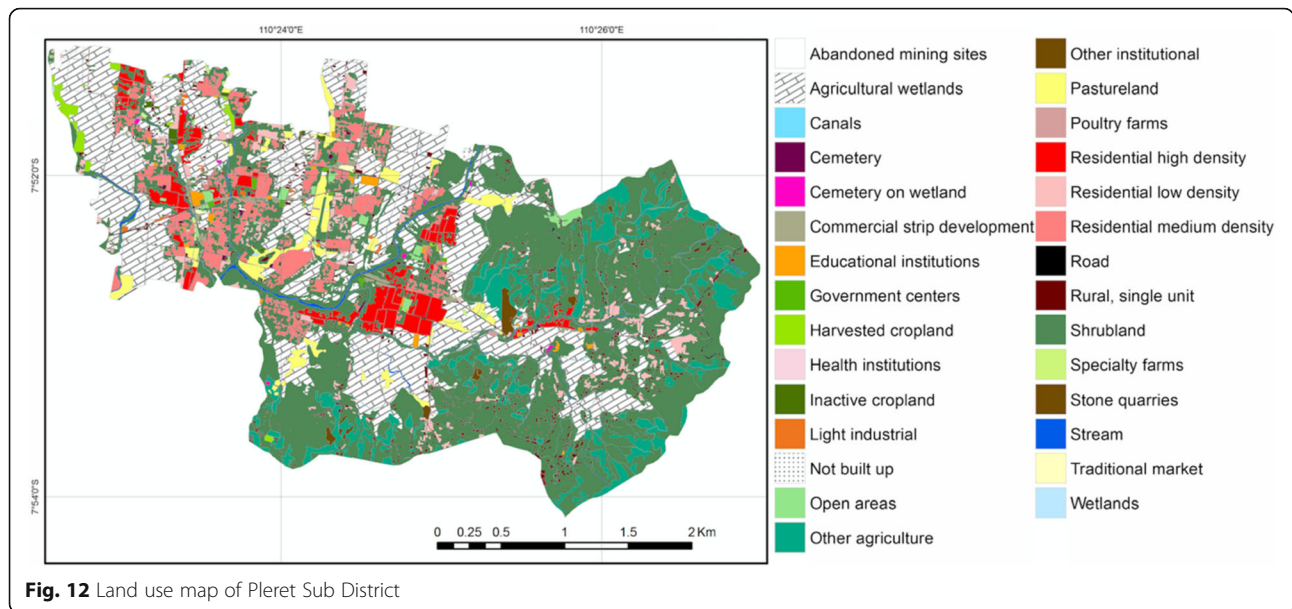


Fig. 12 Land use map of Pleret Sub District

of reinforce masonry, asbestos or zinc roof, located between 10.1 and 12 km from the epicentre, and being located on Semilir Formation, with a probability of not damaged equal to 0.85 or probability of collapse equal to 0.07. Only five buildings or 0.028% of the total buildings in the research area have this building attribute combination. The most vulnerable buildings in the research area are the ones with a combination of reinforced masonry structure, clay tile roof, being located between 8.1 and 10 km from the epicentre, and being located on young Merapi volcanic deposits. This building attribute combination gives a value of collapsed probability equal to 0.84 or not damaged probability equal to 0.07. The number of the buildings with a vulnerable combination is 45 buildings or 0.25% of the total buildings. Most of the buildings in research area have a combination of reinforced masonry, clay tile roof, are located more than 12 km from the epicentre, and are located on young Merapi volcanic deposits (37.71%). This building attribute combination gives the collapse probability value of 0.67 and it is predicted as highly damaged building or collapsed. The building foot print model of building damage probability is shown in the Fig. 13.

The scenario of minimum, maximum, and average damage was also applied to generalise the building foot print model into the building block probability. The conversion method follows the illustration shown in Fig. 7 above. We found that the pattern of probability value

Table 9 Model fit information

Model	-2 Log Likelihood	Chi-Square	df	Sig.
Intercept Only	3055.003			
Final	707.190	2347.813	11	.000

Link function: Logit

between minimum, maximum, and average scenarios were slightly different. Based on the minimum scenario, the building block located on the western part of Opak river has a probability of collapse between 0.22 and 0.81, while based on the maximum and average scenarios, probability of collapse is the same, about 0.29–0.81. The rest of the building located in eastern part of Opak river has collapsed probability value about 0.07–0.84; 0.08–0.84; and 0.08–0.84 of minimum, maximum, and average scenarios, respectively. The complete map of the collapsed probability and the predicted building damage categories under minimum, maximum, and average scenarios are shown in the Fig. 14 and Fig. 15.

Population distribution

The population distribution analysis was applied to disaggregate the number of people at Sub District level into a particular land use types within the area. The temporal analysis of population distribution based on the types of occupation was also conducted in this stage. The main concept of this analysis is to breakdown the population data using dasymetric technique. The main equation used follows the equations 1, 2 and 3 above. The characteristic of livelihood of each village was also used to support the analysis. The result shows that the top 5 occupation types in research area are casual worker, student, unemployment, entrepreneur, and farmer. The percentage of people

Table 10 Pseudo R-square

Cox and Shell	.264
Nagelkerke	.332
McFadden	.194

Link function: Logit

Table 11 Parameter estimates

		Estimate	Std. Error	Wald	df	Sig.	95% Confidence Interval	
							Lower Bound	Upper Bound
Threshold	[Damage = 1]	1.529	.478	10.247	1	.001	.593	2.465
	[Damage = 2]	2.426	.478	25.761	1	.000	1.489	3.363
Location	[Structure = 0]	-.255	.107	5.647	1	.017	-.465	-.045
	[Structure = 1]	.685	.070	95.306	1	.000	.547	.822
	[Structure = 2]	0 ^a	.	.	0	.	.	.
	[Roof = 0]	.430	.610	.497	1	.481	-.766	1.627
	[Roof = 1]	.749	.484	2.390	1	.122	-.201	1.698
	[Roof = 2]	1.634	.461	12.541	1	.000	.729	2.538
	[Roof = 3]	0 ^a	.	.	0	.	.	.
	[Distance = 1]	2.265	.236	91.712	1	.000	1.801	2.728
	[Distance = 2]	.949	.106	80.173	1	.000	.742	1.157
	[Distance = 3]	.744	.084	78.154	1	.000	.579	.909
	[Distance = 4]	0 ^a	.	.	0	.	.	.
	[Geology = 0]	-1.413	.122	134.395	1	.000	-1.652	-1.174
[Geology = 1]	-.640	.145	19.402	1	.000	-.925	-.355	
[Geology = 2]	1.507	.117	165.861	1	.000	1.278	1.737	
[Geology = 3]	0 ^a	.	.	0	.	.	.	

Link function Logit

^aThis parameter is set to zero because it is redundant

who work as casual workers reaches 17.92%; 20.51%; 18.86%; 20.16%; and 23.99% in Wonokromo, Pleret, Segoroyoso, Bawuran and Wonolelo Village, respectively. The percentage of the students of every village are 16.03%; 13.89%; 12.60%; 11.55%; and 9.89%. The unemployed people percentage reaches approximately 13.69%; 12.89%; 12.88%; 13.32%; 12.11% and the entrepreneurs

approximately 11.84%; 12.88%; 16.72%; 16.12%; 9.55%. The farm workers only reach 8.86% in Wonokromo, 11.03% in Pleret, 12.17% in Segoroyoso, 13.59% in Bawuran, and 15.18% in Wonolelo.

Based on the population percentage calculation of each land use type, during the working hour the population is scattered into three major land use types such as

Table 12 The example of the calculation of predicted damage categories

No	Freq	Str	Rf	Dist	Geo	Structure			Roof				Distance				Geology				Sum (Y*)	DC
						Str 0	Str 1	Str 2	Rf 0	Rf 1	Rf 2	Rf 3	Dst 1	Dst 2	Dst 3	Dst 4	Geo 0	Geo 1	Geo 2	Geo 3		
1	22	0	2	2	0	-0.255	0	0	0	0	1.634	0	0	0.949	0	0	-1.413	0	0	0	0.915	1
2	3	0	2	2	1	-0.255	0	0	0	0	1.634	0	0	0.949	0	0	0	-0.64	0	0	1.688	2
3	1	0	2	3	0	-0.255	0	0	0	0	1.634	0	0	0	0.744	0	-1.413	0	0	0	0.71	1
4	37	0	2	3	2	-0.255	0	0	0	0	1.634	0	0	0	0.744	0	0	0	1.507	0	3.63	3
5	66	0	2	4	2	-0.255	0	0	0	0	1.634	0	0	0	0	0	0	0	1.507	0	2.886	3
6	1	1	2	2	3	0	0.685	0	0	0	1.634	0	0	0.949	0	0	0	0	0	0	3.268	3
7	25	2	0	2	0	0	0	0	0.43	0	0	0	0	0.949	0	0	-1.413	0	0	0	-0.034	1
8	30	2	0	2	1	0	0	0	0.43	0	0	0	0	0.949	0	0	0	-0.64	0	0	0.739	1
9	10	2	0	2	2	0	0	0	0.43	0	0	0	0	0.949	0	0	0	0	1.507	0	2.886	3
10	1	2	0	2	3	0	0	0	0.43	0	0	0	0	0.949	0	0	0	0	0	0	1.379	1

n = 33

Freq: Frequency; Str: Structure; Rf: Roof; Dist: Distance from the epicentre of the Yogyakarta earthquake 2006; Geo: Geology; Str 0: Wood structure; Str 1: Unreinforced masonry; Str 2: Reinforced masonry; Rf 0: Asbestos or zinc roof; Rf 1: Cement tile roof; Rf 2: Clay tile roof; Rf 3: Concrete slab roof; Dst 1: within 8 km from the epicentre; Dst 2: between 8.1 and 10 km; Dst 3: between 10.1 and 12 km; Dst 4: Between 12.1 and 15 km; Geo 0: Semilir Formation; Geo 1: Alluvium; Geo 2: Young Merapi volcanic deposits; and Geo 3: Nglanggran Formation

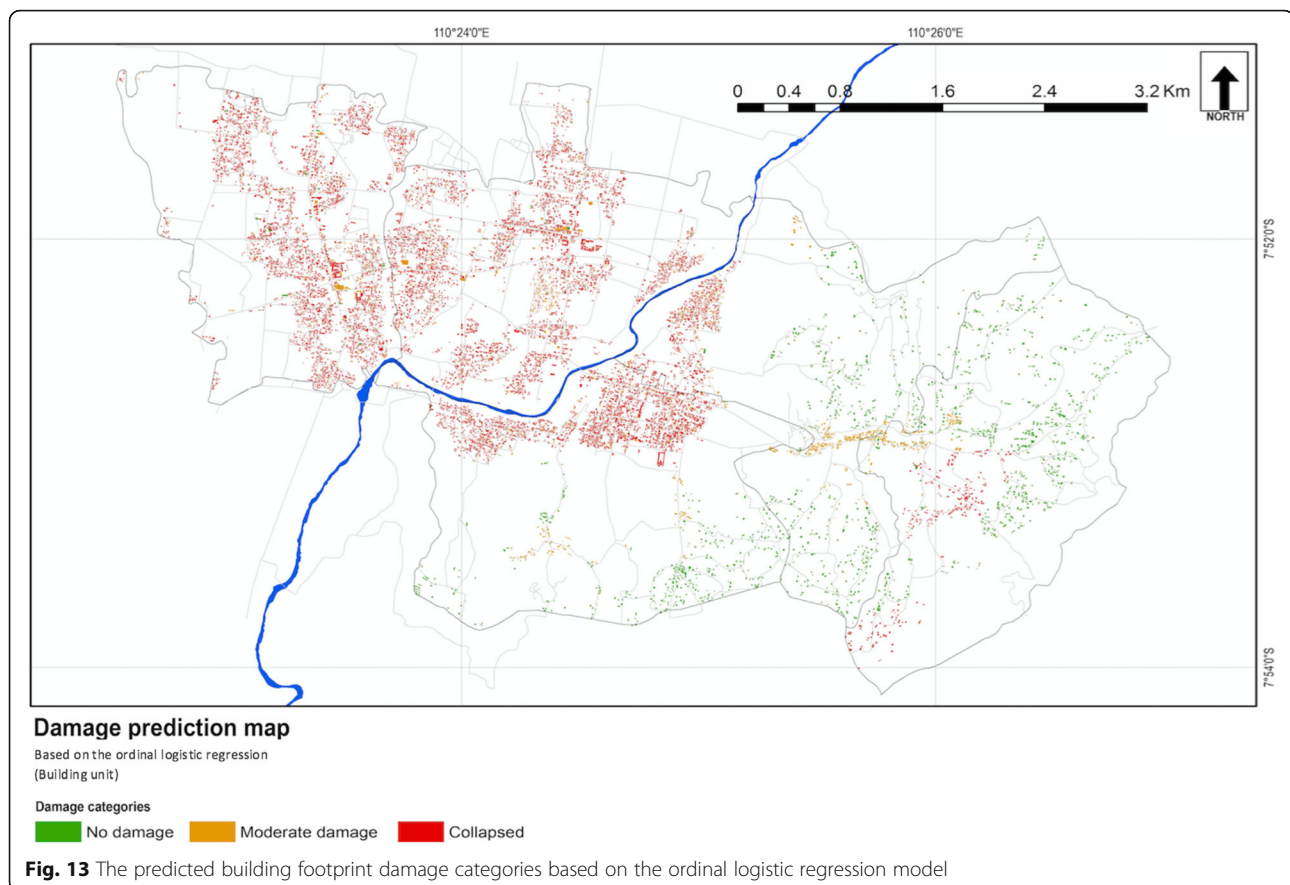
Table 13 The probability calculation and results

No	Y*i	A 1 + e^(Y*i-Tr1)	B 1/A	C Pr#1	D 1 + e^(Y*i-Tr2)	E 1/D	F pr#2 (E-C)	G pr#3 (1-E)
1	0.915	1.54122	0.64884	0.64884	1.22072	0.81919	0.17035	0.18081
2	1.688	2.17232	0.46034	0.46034	1.47811	0.67654	0.21620	0.32346
3	0.71	1.44091	0.69401	0.69401	1.17982	0.84759	0.15358	0.15241
4	3.63	9.17256	0.10902	0.10902	4.33301	0.23079	0.12177	0.76921
5	2.886	4.88398	0.20475	0.20475	2.58400	0.38700	0.18225	0.61300
6	3.268	6.69062	0.14946	0.14946	3.32080	0.30113	0.15167	0.69887
7	-0.034	1.20954	0.82676	0.82676	1.08546	0.92127	0.09451	0.07873
8	0.739	1.45388	0.68781	0.68781	1.18511	0.84381	0.15599	0.15619
9	2.886	4.88398	0.20475	0.20475	2.58400	0.38700	0.18225	0.61300
10	1.379	1.86072	0.53743	0.53743	1.35103	0.74018	0.20275	0.25982
11	-0.239	1.17071	0.85419	0.85419	1.06962	0.93491	0.08073	0.06509
12	0.534	1.36976	0.73005	0.73005	1.15080	0.86896	0.13891	0.13104
3	2.251	3.05839	0.32697	0.32697	1.83947	0.54363	0.21666	0.45637
14	1.174	1.70120	0.58782	0.58782	1.28597	0.77762	0.18980	0.22238
15	1.937	2.50374	0.39940	0.39940	1.61327	0.61986	0.22046	0.38014
16	2.256	3.06871	0.32587	0.32587	1.84368	0.54239	0.21652	0.45761
17	2.486	3.60361	0.27750	0.27750	2.06183	0.48501	0.20751	0.51499
18	1.17	1.69840	0.58879	0.58879	1.28483	0.77831	0.18952	0.22169
19	1.943	2.51279	0.39796	0.39796	1.61696	0.61844	0.22048	0.38156
20	4.09	13.94532	0.07171	0.07171	6.27948	0.15925	0.08754	0.84075
21	2.583	3.86879	0.25848	0.25848	2.16998	0.46083	0.20236	0.53917
22	0.965	1.56896	0.63736	0.63736	1.23204	0.81166	0.17430	0.18834
23	1.738	2.23242	0.44794	0.44794	1.50262	0.66551	0.21756	0.33449
24	3.885	11.54610	0.08661	0.08661	5.30101	0.18864	0.10203	0.81136
25	2.378	3.33710	0.29966	0.29966	1.95314	0.51200	0.21234	0.48800
26	0.221	1.27040	0.78716	0.78716	1.11028	0.90068	0.11352	0.09932
27	3.141	6.01199	0.16633	0.16633	3.04404	0.32851	0.16218	0.67149
28	0.309	1.29527	0.77204	0.77204	1.12042	0.89252	0.12048	0.10748
29	2.456	3.52667	0.28355	0.28355	2.03045	0.49250	0.20895	0.50750
30	0.949	1.55993	0.64105	0.64105	1.22836	0.81410	0.17304	0.18590
31	0.104	1.24054	0.80610	0.80610	1.09810	0.91066	0.10457	0.08934
32	2.251	3.05839	0.32697	0.32697	1.83947	0.54363	0.21666	0.45637
33	1.507	1.97824	0.50550	0.50550	1.39896	0.71482	0.20932	0.28518

Pr Probability
 Tr 1 (Threshold 1 = 1.529)
 Tr2 (Threshold 2 = 2.426)
 e = 2.718

commercial area, school, and settlement. In Wonokromo Village about 27.7% of people are in a commercial area, 16.65% are in school, 16.47% are in a settlement and the rest of them are scattered in other land use types. In contrast with it, approximately 77.91% people in Wonokromo stay at a settlement in the night time, while during holidays, the percentage people who stay at a settlement are 56.29% and this

increases to 87.32% in the night time. Similar with Wonkromo Village, the other four villages have the same pattern. During the working hours, commercial areas, schools, settlements, and agricultural areas tend to become densely populated and this decreases during night time or holidays. The map of population distribution under several scenarios can be seen in Fig. 16, 17, 18, and 19.



The final result, multi-vulnerability of building blocks, is obtained by combining the population distribution model and the predicted building damage categories. The results (Fig. 20 and 21) show that the western and middle part of the research area are dominated by moderate and high levels of vulnerability, while the eastern parts are dominated by low levels of vulnerability. The vulnerability patterns of working hours and holiday times are not considerably different. However, the vulnerability level of some settlement blocks are increasing during night and holiday times.

Model validation

Several validation tests have been conducted in this study. First, a validation of geological unit interpretation, second, a validation of building structure, and last, a validation of the predicted building damage categories. The validation of geological units shows that 72 fieldwork locations have the same geological characteristic with the information of geological map used in this study (Fig. 9 and 10). This result indicate that the interpretation is accurate and it can be used for further analysis.

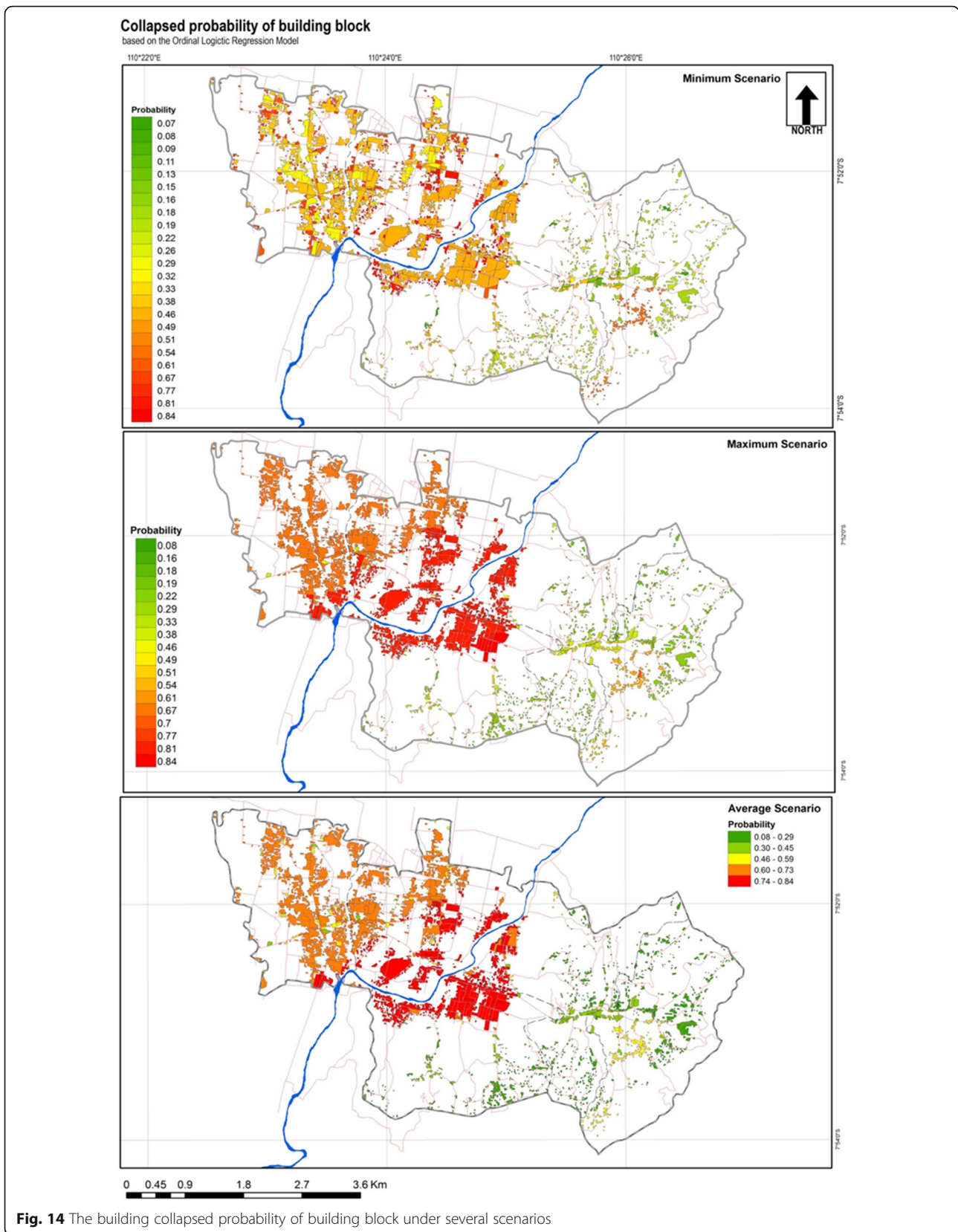
The building structure validation using confusion matrix analysis shows that the visual interpretation of building structure is highly accurate. The accuracy level

of interpretation from the total of 332 buildings sample is 95.18% (Table 14). This result also indicate that the interpretation result of building structure is accurate and it can be used for further analysis.

The last part of the validation process was to calculate the accuracy level of the ordinal logistic regression model. The main calculation was to compare and calculate the matching value between the response variable (building damage) and the predicted damage categories. The result shows that, the ordinal logistic regression model was able to predict precisely the response variable for about 5,795 out of 7,645 building damage data points or about 75.80% of the total. This means that the model can predict accurately the building damage. Additionally, this model can be applied to a dataset of another area of interest. Table 15 below shows an example of the model validation process.

Discussion

The visual interpretation results of Landsat 7 ETM+ produced a 1:40.000 geological map which is slightly different from the existing geological map produced by (Rahardjo et al. 1995). The main distinctions are 1) the border between Semilir Formation and Nglanggran Formation in the Baturagung escarpment, 2) the border



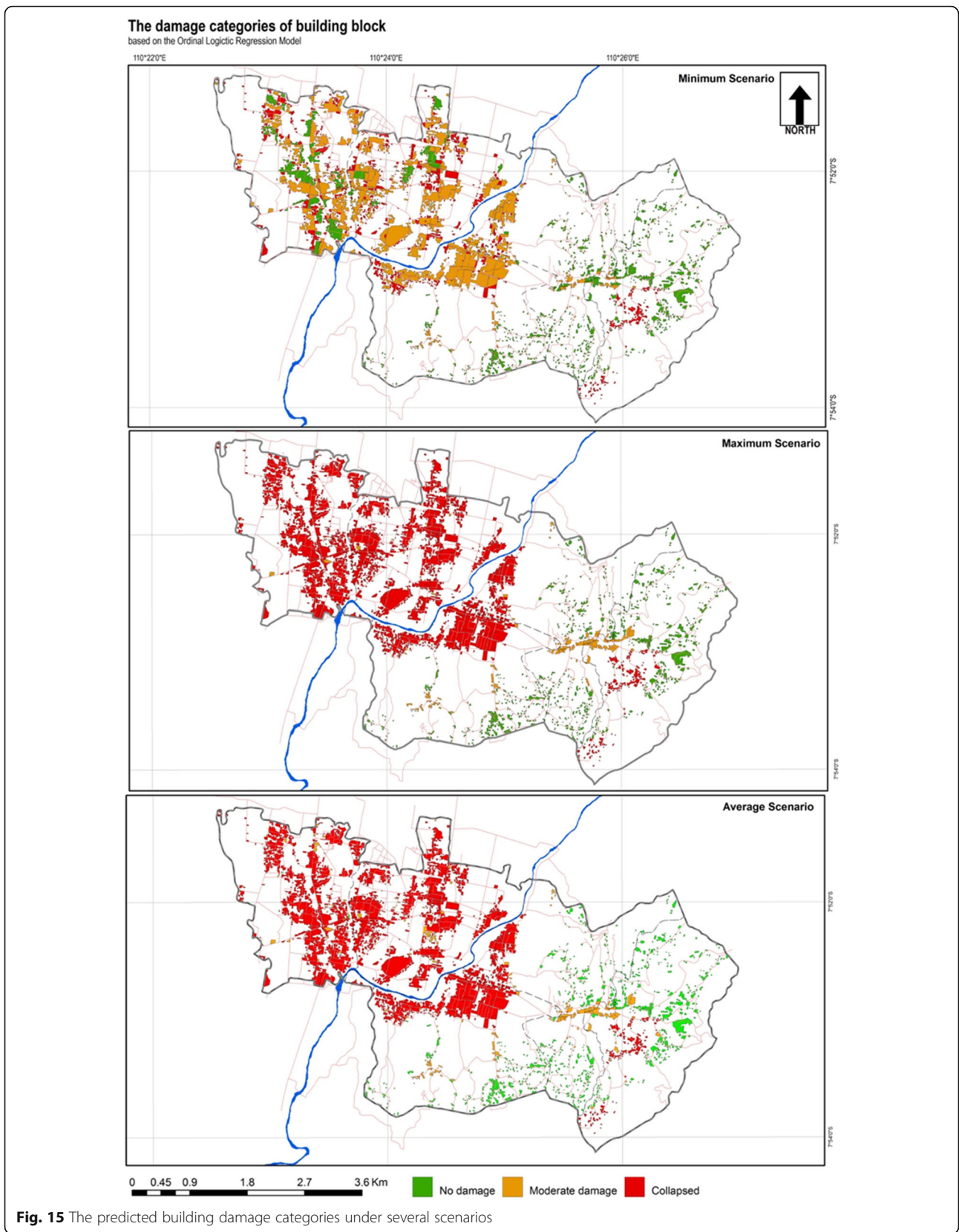


Fig. 15 The predicted building damage categories under several scenarios

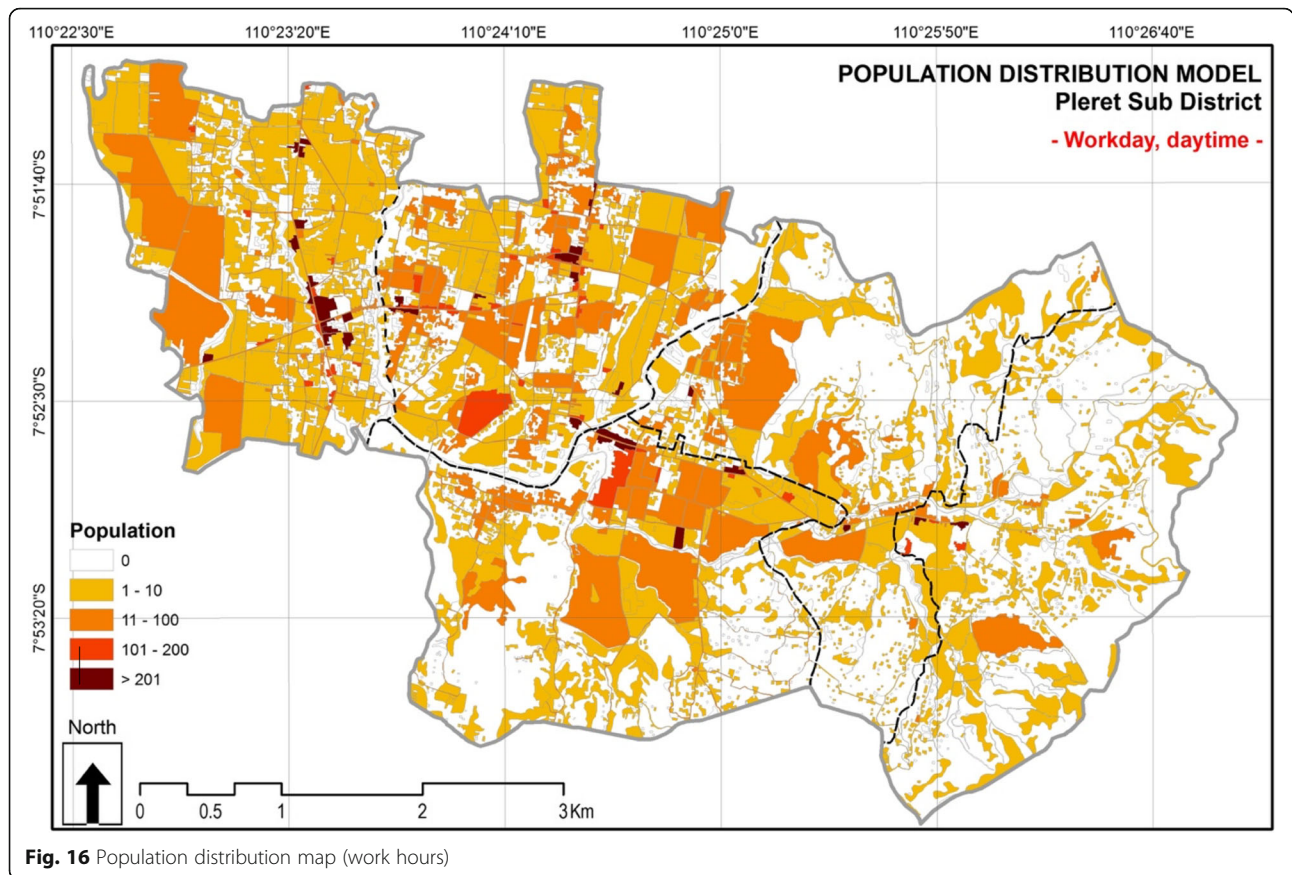


Fig. 16 Population distribution map (work hours)

between young volcano deposits of Merapi Volcano and alluvium, 3) and the isolated hill member of Nglanggran formation (*G.Gelap*) which does not exist in the geological map of Yogyakarta. Based on the interpretation results and field work validation, we found that the border between Semilir and Nglanggran Formation is located on the upper slope of Baturagung, while according to the Geological map of Yogyakarta, the border is located in the middle slope of Baturagung. We found also two isolated hills in the west part of Opak river namely *Gunung Gelap*. This result is very similar to the Sanjoto (2004) results. They found also two isolated hills in the same location which consist of volcanic breccia, flow breccia, agglomerate, lava and tuff members of Nglanggran Formation (Fig. 9). By combining the Yogyakarta map with the geological map resulted from interpretation process, a better understanding of the local geological characteristics can be obtained, which is important for further analysis.

The Yogyakarta earthquake in 2006 caused a major impact to the local infrastructure, especially in the housing sector. Scientists believe that the damage pattern is controlled by certain factors. Qualitative, semi-qualitative, and quantitative methods have been developed to model the controlling factors. Some

studies have been conducted to get a better understanding about the damage pattern caused by the Yogyakarta earthquake in 2006, such as the study conducted by Nurwihastuti, et al. (2014). The study concludes that there is connection between earthquake damage pattern, geomorphological characteristics and sub-surface characteristics. They found that the severe damage tends to occur in areas that have deep basement, low gravity anomaly, thick sediment, and unconsolidated material, while the slight damages tend to occur in areas that have shallow basement, high gravity anomaly, thin sediment, and consolidated material. These results are also in accordance with the previous study conducted by (Daryono, 2011). They found that the high vulnerability of seismic index (*kg*), tends to give a major impact on buildings and infrastructures. This area covers the west part of research area which consists of young volcanic deposits of Merapi volcano and alluvium.

The aforementioned studies allowed for a better understanding on how to characterize the pattern of damage caused by The Yogyakarta earthquake in 2006. However, the scope of those studies, explain only the physical characteristics. Therefore, the probabilistic modelling for estimating earthquake vulnerability was

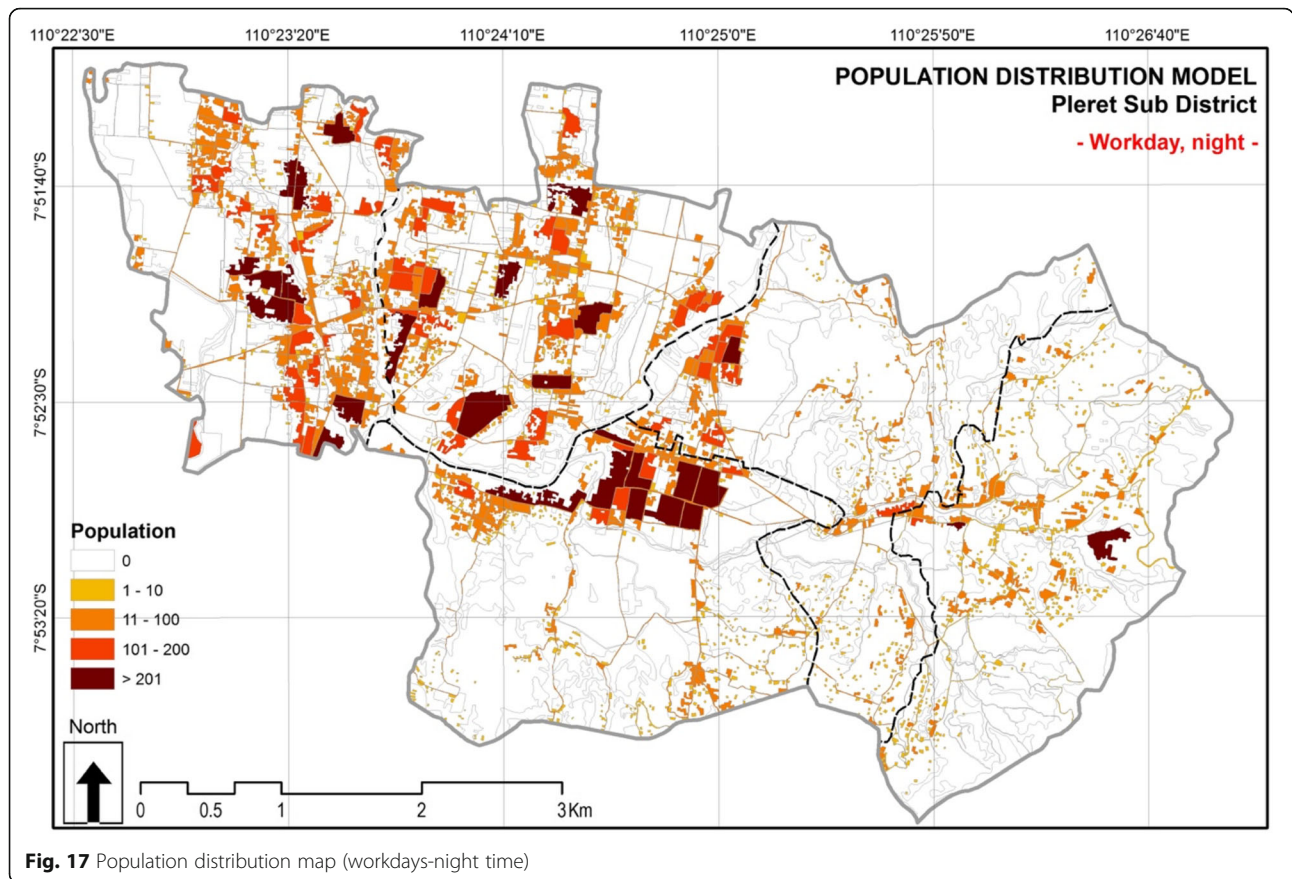


Fig. 17 Population distribution map (workdays-night time)

conducted to provide further understanding of the problem. For this, we used an integrated analysis methodology using remote sensing, GIS analysis and statistical modelling. A combination of physical and building characteristics was used as the independent variables. These were the type of building structure, roof type, distance to the epicentre, and geological characteristics. As mentioned in the results chapter, the model was able to explain the probability of building damage with a 75.80% success rate. This model shows that the combination of reinforced masonry structure, clay tile roof, being located between 8.1 and 10 km from the epicentre, and being located on young Merapi volcanic deposits defines the most vulnerable type of building in the study area.

Most of the existing reinforced masonry buildings in the research area consist of three main structure components such as the building foundation, reinforced concrete columns, and roof structure. Sometimes the buildings have no ground beam and roof beam, which implies lack of connection between roof, concrete columns, and roof structure. Moreover, they have no diagonal concrete columns which are useful to reduce the tensile stresses during a seismic vibration. The use of clay tile in this case, will increase also the probability of

a collapse. As shown in the Table 11, clay tile roof has a value of 1.634, which means that clay gives the higher probability of a collapse (equal to 1.634) compared to the roof benchmark (concrete slab). In fact, it has a heavier weight (1.49 kg per square meter) than asbestos and concrete tile or cement tile. The distance from the epicentre also contributes to the probability of collapse. According to the model, the further from the epicentre, the lower the probability of damage.

The young volcanic deposits of Merapi Volcano give also the highest contribution to the probability of building collapse among the other geological units. This unit is characterized as deep basement, thick sediment, unconsolidated material and having abundant shallow groundwater. The area has high possibility of ground amplification occurrence (Daryono, 2011) (Nurwihastuti et al., 2014) (Koseki, et al., 2007) (Pandita et al. 2016). Parallel with the result of Nurwihastuti, et al. (2014), most collapsed buildings due to The Yogyakarta earthquake were located in fluvial landforms, in this case the fluvial plain that consist of Young Merapi volcano deposits. The probabilistic model also shows that the usage of ordinary reinforced masonry and clay tile is not suitable in this area. it estimates that the combination of

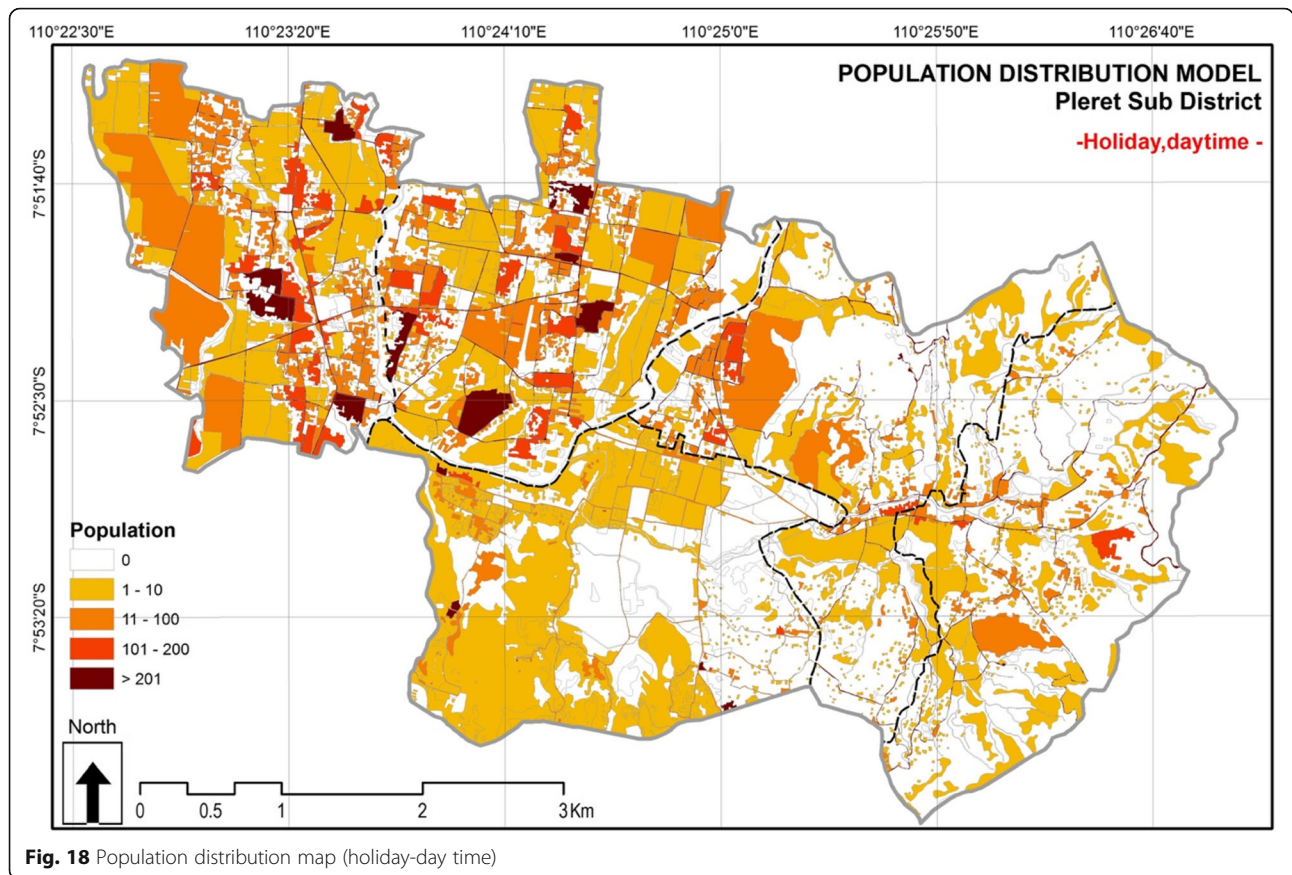


Fig. 18 Population distribution map (holiday-day time)

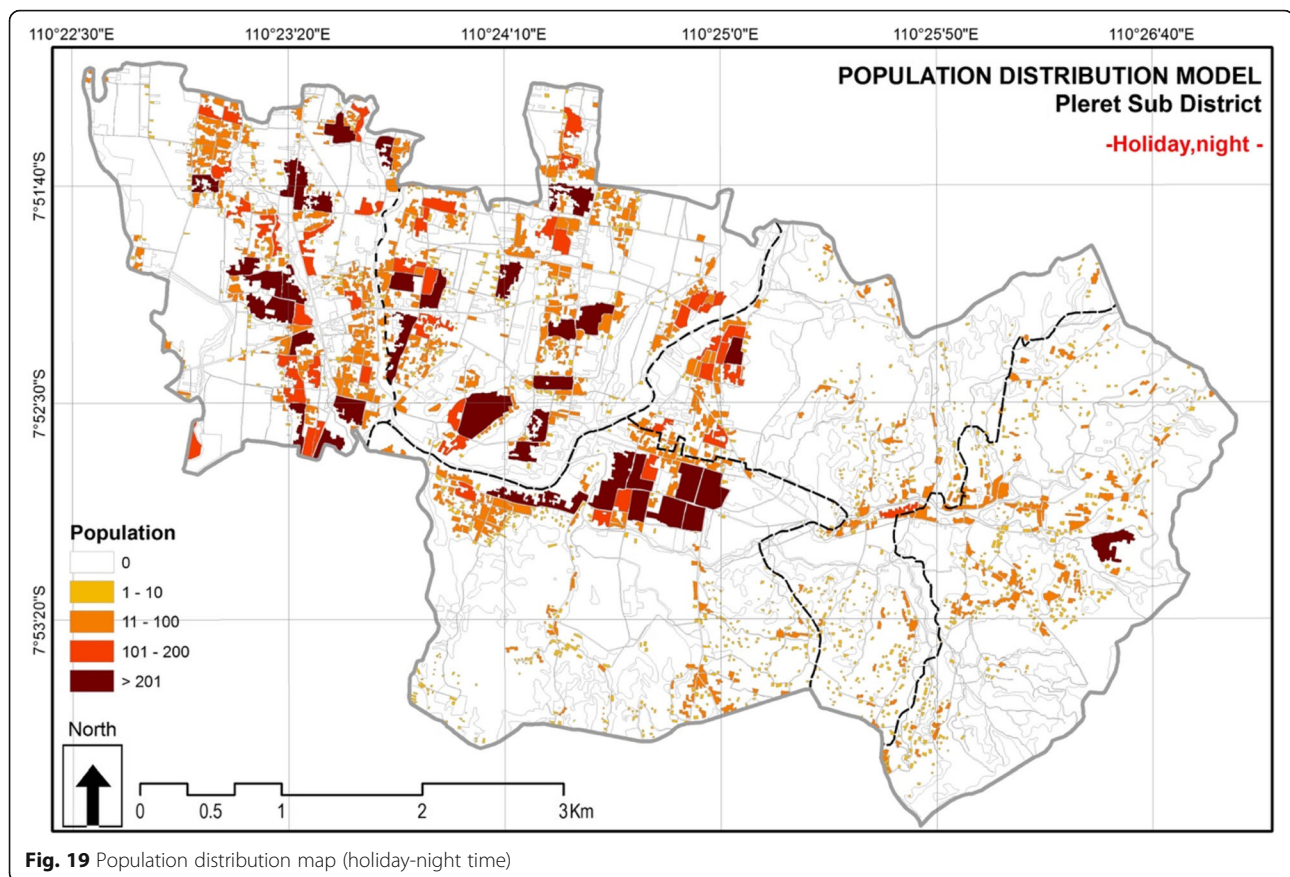
structure and roof material types in this zone gives a probability of collapse between 0.51 and 0.84. Thus, it is recommended to build a house by using the building structure of wood and light steel roof or reinforced masonry with a good connection between foundation, concrete column, and roof structure.

However, the combination of reinforced masonry, asbestos zinc, and being located in Semilir Formation gives the lowest probability of collapse in the model. This is because the Semilir Formation is a massive volcanic rock which consists of interbedded tuff breccia, pumice breccia, dacite tuff, andesite tuff, and tuffaceous clay stone. This rock formation can reduce the ground amplification caused by an earthquake. In line with Daryono (2011) results, the lowest value of seismic index vulnerability is located in the structural and denudational landform member of Semilir Formation.

This probabilistic method is very suitable for developing countries like Indonesia where a national standard of building code and map of building damage prediction are less available. It provides a comprehensive and simple probabilistic modelling of building damage which can be used easily by scientists and decision makers at both local and regional levels to improve the current

disaster and risk management reduction programs. By using this method, an accurate results of preliminary damage prediction up to 75% level of correctness can be provided with relatively limited time and cost.

There are several limitations that need to be taken into consideration for future research and improvement of the model. Within this study, only few variables were used in the ordinal logistic regression. Only about 33.20% of the model can explain the variance. There still is about 66.80% that might be explained by other factors. However, the model fit information (Table 9) showed the significant result. It means, this model is appropriate and can be used for further analysis, although the model only can explain of 33.20% of variance. Thus, the advanced study with more additional independent variable is needed to improve the results and to gain higher level of variance explanation. In term of engineering purposes, a detailed investigation of residential building is absolutely need to be conducted to determine the safety factor and vulnerability of the buildings. Based on the main requirement on how to build the safer houses, which was recommended by the Indonesian Ministry of Public Works, there are some aspects that determine the vulnerability of the buildings. First, a good



quality of construction material. Second, appropriate structural existence and dimension. Third, a good connection within the main structural elements, and fourth, a good processing quality. Additionally, for the Joglo houses, the quality of the timber (age, type of the material, quality of the carpentry, and maintenance) also determines the level of earthquake vulnerability. Thus, for further research the combination of this probabilistic model and the detailed site investigation are very important to support the existing building code.

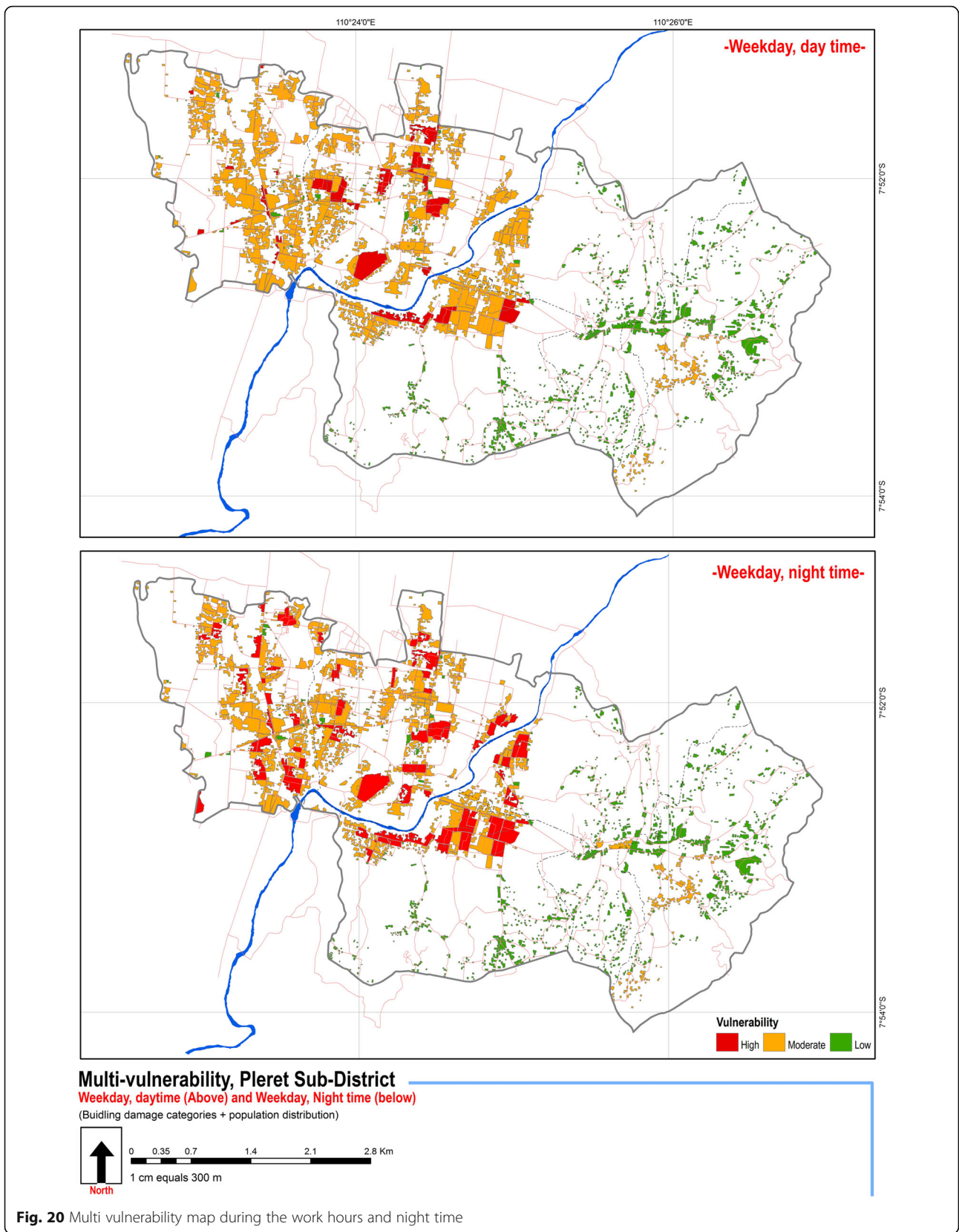
The others research that can be carried out in the future is the study about the outcrop or geological mapping activities. By improving the geological map of Yogyakarta 1: 100,000; the better understanding of geological characteristic and surface material behaviour during the earthquake can be obtained. Moreover, the outcrop study is able to reconstruct the minor fault which was unidentified from the geology map of Yogyakarta. By revealing the configuration of this minor faults, the collateral damages due to amplification of the fault can be avoided.

Further research also needs to be done to model the population distribution in space and time. This study only used a percentage analysis to disaggregate the

population data at a Village level into particular land use types. This model gives only a general description about how the population spreads in time based on their livelihood type. A good local knowledge and local community habit understanding are absolutely necessary to generate this model. Therefore, primary data of population distribution are very important to explain the patterns of local community behaviour. However, this model provides a valuable information for the local government to support decision making concerning earthquake hazards and risk management.

Conclusion

Earthquake hazard becomes a serious problem in Java and particularly in Southern Java as a result of the subduction zone along the south part of the area, about 320 km south of Yogyakarta. In addition, there is a growing demand for residential buildings due to the rapid population growth. This condition might lead to a higher level of vulnerability to earthquake disaster. This phenomenon has triggered scientists to further study and model the corresponding earthquake hazards, vulnerability, and make risk assessments to help reduce disaster risks. Several



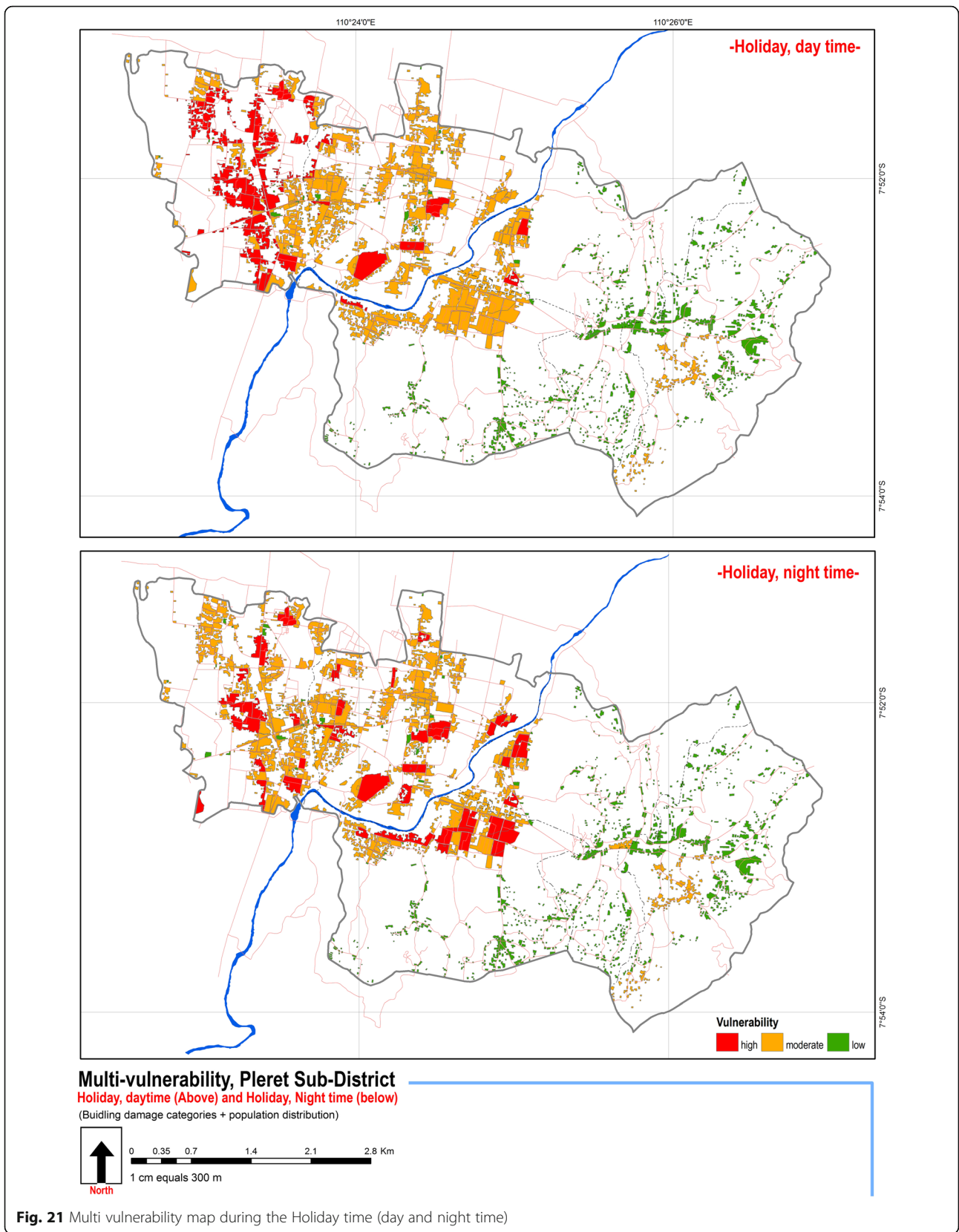


Table 14 Confusion matrix analysis of the building structure

Interpretation	field work data (2012)			total
	Reinforced masonry	Unreinforced masonry	Wood	
Reinforced masonry	302	1	5	308
Unreinforced masonry	0	0	0	0
Wood	10	0	14	24
total	312	1	19	332

Diagonal sum : 316
 Diagonal sum/ grand total: 0.951
 Accuracy: 95.18%

studies have been conducted to analyse the damage patterns caused by The Yogyakarta earthquake in 2006. By combining the geophysical and building characteristics, this study provides an accurate prediction about 75.81% of building damage probability. Based on the results of an ordinal logistic regression model, the reinforced masonry house with clay tile roof, it is located between 8.1 and 10 km from the epicentre of the 2006 earthquake and was built on young Merapi volcanic deposits has higher probability of building damaged. On the contrary, the combination of reinforced masonry, asbestos or zinc roof, being located in Semilir Formation and far (>12 Km) from the 2006 epicentre has lower probability of buildings damaged. Additionally, the results explain the estimation or prediction of building vulnerability based on the building damaged of the Yogyakarta earthquake 2006. This study is also suitable for preliminary study at the regional scale. Thus, the site investigation still needs to be conducted for the future research to determine the safety and vulnerability of residential building.

Table 15 The validation of ordinal logistic regression model

Building ID	Damage	Ordered Logit Prediction	Correctly classified
30	3	3	1
31	3	3	1
32	3	3	1
33	3	3	1
34	3	3	1
35	3	3	1
36	3	3	1
37	3	3	1
38	3	3	1
39	3	1	0
40	3	1	0

n 7,645

Sum correct 5,795

% correct 75.80

Acknowledgement

This paper is part of the PhD research at Dept. of Geography, University of Canterbury, New Zealand, which is funded by the Indonesia Endowment Fund for Education (LPDP-Indonesia). The author is thankful to main supervisor, Dr. Christopher Gomez, who has supported this project, co supervisor Dr. Ioannis Delikostidis, Dr. Danang Sri Hadmoko and Prof. Dr. Junun Sartohadi. We also acknowledge the University of Canterbury New Zealand who provided adequate reference for this project.

Authors' contribution

AS and CG collected the data, AS carried out the analysis of coseismic landslide, CG and ID support on the interpretation of the results. TR support on the analysis of building vulnerability and MDR support on the statistical analysis. AS drafted the manuscript, CG, DSH and JS revised the manuscript. All the authors drafted, read and approved the final manuscript.

Competing interests

The authors declare that they have no competing interests.

Publisher's Note

Springer Nature remains neutral with regard to jurisdictional claims in published maps and institutional affiliations.

Author details

¹Department of Geography, University of Canterbury, Private Bag 4800, Christchurch, New Zealand. ²Geography Faculty, Universitas Muhammadiyah Surakarta, Central Java, Indonesia. ³Department of Civil Engineering, Politeknik Negeri Malang, East Java, Indonesia. ⁴Faculty of Agribusiness and Commerce, Lincoln University, Lincoln, New Zealand. ⁵Institute for Economics and Social Research, University of Indonesia (LPEM-UI), Jakarta, Indonesia. ⁶Department of Environmental Geography, Geography Faculty, Universitas Gadjah Mada, Yogyakarta, Indonesia. ⁷Research Centre of Volcanic Risk at Sea, Faculty of Maritime Sciences, University of Kobe, Kobe, Japan.

Received: 2 December 2016 Accepted: 15 March 2017

Published online: 24 March 2017

References

- Abidin, H, H Andreas, I Meilano, M Gamal, I Gumilar, and C Abdullah. 2009. Deformasi koseismik dan pascaseismik gempa Yogyakarta 2006 dari hasil survei GPS. *Jurnal Geologi Indonesia* 4: 275–284.
- Aswandono, B. 2011. Building replacement cost for seismic risk assessment in Plabapang Village, Bantul Sub-District, Yogyakarta Indonesia, Master's Thesis. Yogyakarta: Universitas Gadjah Mada.
- BAPPENAS. 2006. The Provincial and Local Government of D.I. Yogyakarta, the Provincial and Local Government of Central Java and International Partners. Preliminary damage and loss assessment: Yogyakarta and Central Java natural disaster. Available via the world bank. <http://documents.worldbank.org/curated/en/2006/06/8180293/preliminary-damage-loss-assessment-yogyakarta-central-java-natural-disaster>. Accessed 1 June 2016.
- Bath, M. 1979. Introduction to seismology, 2nd ed. Basel: Birkhauser.
- Bawuran Village. 2014. Data pekerjaan. <http://bawuran.bantulkab.go.id/index.php/first/statistik/1>. Accessed 10 Sept 2016.
- BPS-Statistics of Bantul Regency. 2010. Kecamatan Pleret dalam angka 2010. Yogyakarta: Statistical Coordinator in Pleret Sub-District.
- BPS-Statistics of Bantul Regency. 2014. Kecamatan Pleret dalam angka 2014. Available via Statistics of Bantul Regency. https://bantulkab.bps.go.id/ipds@3402/pdf_publicasi/Kecamatan-Pleret-Dalam-Angka-2014.pdf. Accessed 30 May 2016.
- Bronto, S, S Mulyaningsih, G Hartono, and B Astuti. 2009. Waduk Parangharjo dan Songputri: Alternatif sumber erupsi Formasi Semilir di daerah Eromoko, Kabupaten Wonogiri, Jawa Tengah. *Jurnal Geologi Indonesia* 4: 77–92.
- Daryono. 2011. Indeks kerentanan seismik berdasarkan mikrotremor pada setiap satuan bentuklahan di zona Graben Bantul Daerah Istimewa Yogyakarta. Dissertation. Yogyakarta: Universitas Gadjah Mada.
- Demets, C, D Gordon, and Stein S Argus. 1994. Effect of recent revisions to the geomagnetic reversal time scale on estimates of current plate motions. *Geophys* 21: 2191–2194.
- Earthquake Engineering Research Institute (ERRI). 2006. The 6.3 Mw Java, Indonesia, Earthquake of May 27, 2006. Available via Earthquake Engineering Research Institute. <https://www.eeri.org/products-publications/eeri-newsletter>. Accessed 29 May 2015.

- Elnashai, A, SJ Kim, GJ Yun, and D Sidarta. 2006. The Yogyakarta earthquake of May 27, 2006. Illinois: Available via Mid-America Earthquake Center. <http://mae.cee.illinois.edu/publications/reports/Report07-02.pdf>. Accessed 30 May 2015.
- FEMA. 2015. Rapid visual screening of buildings for potential seismic hazards: a handbook (3 ed.) FEMA P-154. Washington DC: Available via Federal Emergency Management Agency. https://www.fema.gov/media-library-data/1426210695633-d9a280e72b32872161efab26a602283b/FEMAP-154_508.pdf. Accessed 1 Jan 2017.
- Freire, S, C Aubrecht, and S Wegscheider. 2013. Advancing tsunami risk assessment by improving spatio-temporal population exposure and evacuation modeling. *Natural Hazard* 68: 1311–1324.
- Irsyam, M, W Sengara, F Aldiamar, S Widiyantoro, W Triyoso, DH Natawidjaja, E Kertapati, I Meilano, Suhardjo, M Asrurifak, and M Ridwan. 2010. Ringkasan hasil studi tim revisi peta gempabumi. Available via The United Nations Office for Disaster Risk Reduction (UNISDR). http://www.preventionweb.net/files/14654_AIFDR.pdf. Accessed 1 May 2016.
- Kerle, N. 2010. Sattelite-based damage mapping following the 2006 Indonesia earthquake—How accurate was it? *International Journal of Applied Earth Observation and Geoinformation* 12: 466–476.
- Koseki, J, M Yoshimine, T Hara, T Kiyota, RI Wicaksono, S Goto, and Y Agustian. 2007. Damage survey report on May 27, 2006, Mid Java Earthquake, Indonesia. *Soils and Foundations* 47(5): 973–989.
- Leech, N, K Barret, and G Morgan. 2005. SPSS for intermediate statistics, use and interpretation, Secondth ed. New Jersey: Lawrence Erlbaum Associates, Publishers.
- Mulyaningasih, S, Y Husadani, P Umboro, S Sanyoto, and D Purnawati. 2011. Aktivitas vulkanisme eksplosif penghasil Formasi Semilir bagian bawah di daerah Jetis Imogiri. *Jurnal Teknologi Technoscintia* 4(1): 64–78.
- Nurwihastuti, DW, J Sartohadi, D Mardiatno, U Nehren, and Restu. 2014. *World Journal of Engineering and Technology* 2: 61–70.
- Pandita, H, and Isjudarto A Sukartono. 2016. Geological identification of seismic source at Opak Fault based on stratigraphic sections of Southern Mountains. *Forum Geografi* 31(1): 77–85.
- Pleret Village. 2014. Data pekerjaan. <http://pleret.bantulkab.go.id/index.php/first/statistik/1>. Accessed 10 Sept 2016.
- Prihatmaji, Y, A Kitamori, and K Komatsu. 2012. Traditional Javanese wooden houses (Joglo) damaged by May 2006 Yogyakarta Earthquake, Indonesia. *International Journal of Architectural Heritage* 8(2): 247–268.
- Rahardjo, W, and Rosidi H Sukandarrumidi. 1995. Geological map of Yogyakarta sheet Jawa. Bandung: Geological Research and Development Centre.
- Sanjoto, S. 2004. Pengaruh komposisi terhadap kualitas dan pengaruh struktur geologi terhadap breksi pumice Formasi Semilir sebagai bahan bangunan interior daerah Bawuran Kecamatan Pleret, Kabupaten Bantul, Yogyakarta. Yogyakarta: Master Thesis, Universitas Gadjah Mada.
- Saputra, A. 2012. Pengurangan risiko gempabumi melalui evaluasi bangunan tempat tinggal dan lingkungannya di Kecamatan Pleret, Kabupaten Bantul, Master Thesis. Yogyakarta: Universitas Gadjah Mada.
- Schluter, H, C Gaedicke, H Roeser, B Schreckenberger, H Meyer, C Reinchert, Y Djajadihardja, and A Prexl. 2002. Tectonic features of the southern Sumatra-western Java forearc of Indonesia. *Tectonics* 21(5): 1047.
- Segoroyoso Village. 2014. Data pekerjaan.. <http://segoroyoso.bantulkab.go.id/index.php/first/statistik/1>. Accessed 10 Sept 2016.
- Stein, S, and M Wysession. 2003. An introduction to seismology, earthquakes, and earth structure. London: Blackwell.
- Su, M-D, M-C Lin, H-H Hsieh, B-W Tsai, and C-H Lin. 2010. Multi-layer multi-class dasymetric mapping to estimate population distribution. *Science of the Total Environment* 408: 4807–4816.
- U.S. Geological Survey. 2007. Land use cover classification system NJDEP modified Anderson system. Available via Departement of Environmental Protection, Bureau of GIS. <http://www.state.nj.us/dep/gis/digidownload/metadata/lulc02/anderson2002.html>. Accessed 6 Sept 2016.
- Walter TR, Wang R, Zimmer M, Grosser H, Luhr B, Ratdomopurbo A (2007) Volcanic activity influenced by tectonic earthquakes-Static and dynamic stress triggering at Mt Merapi. *Geophysical Research Letters* 34 (5). doi:10.1029/2006GL028710.
- Wijanto S, Sinha R (2003) World housing encyclopedia report. Available via Earthquake Engineering Research Institute (EERI). https://www.eeri.org/lfe/pdf/indonesia_unreinforced_clay.pdf. Accessed 14 January 2016
- Winarti, and HG Hartono. 2015. Ancient volcanic rocks identification the western part of Yogyakarta southern mountains based on geoelectrical measurement. *Eksplorium* 36(1): 57–70.
- Wonokromo Village. 2014. Data pekerjaan. <http://wonokromo.bantulkab.go.id/index.php/first/statistik/1>. Accessed 10 Sept 2016.
- Wonolelo Village. 2014. Data pekerjaan. <http://wonolelo.bantulkab.go.id/index.php/first/statistik/1>. Accessed 12 Dec 2015.
- Yusliandi, A, HG Hartono, and S Bernadeta. 2013. Studi genesis co-ignimbrite daerah Pasekan dan sekitarnya, Kecamatan Eromoko, Kabupaten Wonogiri, Provinsi Jawa Tengah. In *Proceeding of Seminar Nasional ke 8: rekayasa teknologi industri dan informasi*, 32–3. Yogyakarta: Sekolah Tinggi Teknologi Nasional.

Submit your manuscript to a SpringerOpen[®] journal and benefit from:

- Convenient online submission
- Rigorous peer review
- Immediate publication on acceptance
- Open access: articles freely available online
- High visibility within the field
- Retaining the copyright to your article

Submit your next manuscript at ► springeropen.com

Reproduced with permission of copyright owner. Further reproduction prohibited without permission.